

Stratified Learning: A General-Purpose Statistical Method for Improved Learning under Covariate Shift

Maximilian Autenrieth^{1*}, David A. van Dyk¹, Roberto Trotta^{1,2},
David C. Stenning³

^{1*}Department of Mathematics, Imperial College London.

²Department of Theoretical and Scientific Data Science, SISSA (Trieste).

³ Department of Statistics and Actuarial Science, Simon Fraser University.

*Corresponding author. E-mail: m.autenrieth19@imperial.ac.uk;
Contributing authors: d.van-dyk@imperial.ac.uk; rtrotta@sissa.it;
dstennin@sfu.ca;

Abstract

We propose a simple, statistically principled, and theoretically justified method to improve supervised learning when the training set is not representative, a situation known as covariate shift. We build upon a well-established methodology in causal inference, and show that the effects of covariate shift can be reduced or eliminated by conditioning on propensity scores. In practice, this is achieved by fitting learners within strata constructed by partitioning the data based on the estimated propensity scores, leading to approximately balanced covariates and much-improved target prediction. We demonstrate the effectiveness of our general-purpose method on two contemporary research questions in cosmology, outperforming state-of-the-art importance weighting methods. We obtain the best reported AUC (0.958) on the updated “Supernovae photometric classification challenge”, and we improve upon existing conditional density estimation of galaxy redshift from Sloan Data Sky Survey (SDSS) data.

Keywords: Astrostatistics, Bias Reduction, Domain Adaptation, Machine Learning, Propensity Scores

1 Introduction

In supervised learning, when the labeled training (source) data do not accurately represent the unlabeled (target) data, learning models may not generalize well, leading to unreliable target output predictions. Domain adaptation methods aim to obtain accurate target predictions under such domain shift (Pan and Yang, 2009). Domain adaptation scenarios are widespread, and a variety of methods to tackle them have been proposed. Following Kouw and Loog (2019), they can be organized into three categories: feature-based methods (e.g., Pan et al., 2010); inference-based methods (e.g., Liu and Ziebart, 2014); and sample-based approaches, with a focus on importance weighting (e.g., Shimodaira, 2000; Sugiyama et al., 2008; Cortes et al., 2010), mainly in the covariate shift framework, which is our focus. (Section S2 of the Supplement includes additional background.)

Covariate Shift:

Adapting a model trained on unrepresentative source data to accurately predict target data labels requires information about the target data distribution. We consider covariate shift, a common case of domain shift. Specifically, let $\mathcal{X} \subset \mathbb{R}^F$, $F > 0$, be the feature space and \mathcal{Y} the label space with $K > 1$ classes, or a subset of \mathbb{R}^K in multivariate regression with K dependent variables. Different domains are defined as different joint distributions $p(x, y)$ over the same feature-label space $\mathcal{X} \times \mathcal{Y}$ (Kouw and Loog, 2019). We consider a transductive, unsupervised domain adaptation case, where source data $\mathcal{D}_S = \{(x_S^{(i)}, y_S^{(i)})\}_{i=1}^{n_s}$ with n_s labelled samples from the joint distribution p_S (source domain \mathcal{D}_S) available, as well as target data $\mathcal{D}_T = \{x_T^{(i)}\}_{i=1}^{n_t}$ with n_t unlabelled samples from the joint distribution p_T (target domain \mathcal{D}_T). To avoid the trivial case, we assume that $p_S(x, y) \neq p_T(x, y)$. For ease of notation, we implicitly condition on an indicator variable S , with $p_S(x, y) := p(x, y|s = 1)$ representing source data (analogously $p_T(x, y) := p(x, y|s = 0)$ for target data). Covariate shift is a particular domain adaptation problem, where the conditional distribution of the output variable given the predictive covariates is the same for source and target data, but the distribution of source and target covariates differ, i.e., $p_S(y|x) = p_T(y|x)$ but $p_S(x) \neq p_T(x)$ (Moreno-Torres et al., 2012).

Covariate shift commonly occurs if training samples are not selected randomly, but biased in terms of certain covariates. For instance, brighter astronomical objects are more likely to be better observed and therefore included in the training set (Lima et al., 2008; Revsbech et al., 2018). Selection bias has been widely studied in the statistical literature (Heckman, 1979; Little and Rubin, 2019), e.g., when estimating treatment effects via observational studies. The transfer of causal inference techniques to domain adaptation has received more attention in recent years – both fields share the goal of obtaining accurate estimators under distribution shift (Magliacane et al., 2018). We build on this work in the present paper.

Propensity Scores:

The introduction of propensity scores (Rosenbaum and Rubin, 1983, hereafter RR83) was groundbreaking in causal inference for obtaining unbiased treatment effect estimates from confounded, observational data. RR83 define the propensity score as the probability of treatment assignment given the observed covariates. They show that, under certain assumptions, conditional on the propensity scores the treatment and control group have balanced covariates, which allows unbiased treatment effect estimation. Four main methods are used to condition on the propensity scores: inverse probability of treatment weighting (IPTW), using the propensity score for covariate adjustment, matching, and stratification on the propensity scores (RR83; Rosenbaum and Rubin, 1984). Extensive work has been done on best practice and generalization of propensity scores in causal inference, too much to list here, and we refer to Imbens and Rubin (2015) for an overview. Propensity scores have also found wide application to related areas, such as classification with imbalanced classes (Rivera et al., 2014), or fairness-aware machine learning (Calders et al., 2013), among others. In the covariate shift framework, estimated propensity scores are used only implicitly for importance weighting (e.g., Zadrozny, 2004; Kanamori et al., 2009) analogously to IPTW, and for matching to obtain validation data (Chan et al., 2020). There has been no effort, however, to transfer the general methodology.

In the causal inference literature, there is an ongoing debate between the use of weighted estimators and stratification/matching (e.g., Rubin, 2004; Lunceford and Davidian, 2004; Austin and Stuart, 2017). While, under correct specification of the propensity score model, weighting leads to consistent estimation of treatment effects, this might not hold for stratification due to potential residual confounding within strata (Lunceford and Davidian, 2004). However, the bias introduced by stratified estimators is traded with reduced variance compared to weighted estimators (Lunceford and Davidian, 2004). In addition, estimates of the propensity score are less variable than estimates of their reciprocal, or similarly a density ratio (to form weights). A small change in an estimated propensity score that is near zero can lead to a large difference in the computed inverse-propensity weight, causing massive variance in the estimates based on the weights (Lunceford and Davidian, 2004; Austin and Stuart, 2017).

Contribution:

We propose stratified learning (*StratLearn*), a simple and statistically principled framework to improve learning under covariate shift, based on propensity score stratification. We show that, theoretically, conditioning on estimated propensity scores eliminates the effects of covariate shift. In practice, we partition (stratify) the (source and target) data into subgroups based on the estimated propensity scores, improving covariate balance within strata. We show that supervised learning models can then be optimized within source strata without further adjustment for covariate shift, leading to reduced bias in the predictions for each stratum. *StratLearn* is general-purpose, meaning it is in principle applicable to any supervised regression or classification task under any model. We provide theoretical evidence for the effectiveness of *StratLearn*, and demonstrate it in a range of low- and high-dimensional applications. We show that the

principled transfer of the propensity score methodology from causal inference to the covariate shift framework allows the statistical learning community to employ hard-won practical advice from causal inference, e.g., balance diagnostics, propensity score model assessment/selection, etc. (e.g., Rosenbaum and Rubin, 1984; Imai and van Dyk, 2004; Austin et al., 2007; Pirracchio et al., 2014). We stratify to condition on propensity scores instead of using importance weighting to avoid the massive variance associated with the latter. *StratLearn* (stratification) does not use individually estimated propensity score values except to form strata, leading to a more robust method (Rubin, 2004), as demonstrated in our numerical studies.

This article is organized as follows. In Section 2, we formally introduce the target risk minimization task, and summarize related literature on covariate shift, particularly on importance weighting methods. We conclude Section 2 with an overview of propensity scores in causal inference, before developing our new methodology in Section 3. In Section 4, we numerically evaluate our method. In Section 4.2, we apply *StratLearn* to Type Ia supernovae (SNIa) classification, which has attracted broad interest in recent years (Kessler et al., 2010; Boone, 2019). Improving upon Revsbech et al. (2018), *StratLearn* obtains the best reported AUC¹ (0.958) on the updated ‘‘Supernovae photometric classification challenge’’ (SPCC) (Kessler et al., 2010). In Section 4.3, we improve upon non-parametric full conditional density estimation of galaxy photometric redshift (i.e., photo- z) (Izbicki et al., 2017), a key quantity in cosmology. Supplemental Materials (numbers appearing with a prepended ‘S’) provide details complementing the numerical results in Section 4 (Sections S5 and S8), and additional numerical evidence using data from the UCI repository (Dua and Graff, 2017) in Section S7, and a variation of the SPCC data (Kessler et al., 2010) in Section S6. For additional background, we provide a bibliographic note (Section S2), details on related methods (Section S3), data and software used in this paper (Section S4), as well as complementary details of our proposed methodology *StratLearn* (Section S1). *StratLearn* is computationally efficient, easy to implement and readily adaptable to various applications. Our investigations show that *StratLearn* is competitive with state-of-the-art importance weighting methods in lower dimensions and greatly beneficial for higher-dimensional applications.

2 Preliminaries

2.1 Target Risk Minimization:

In a supervised learning task, let $f : \mathcal{X} \rightarrow \mathbb{R}^K$ be the training function, and $\ell : \mathbb{R}^K \times \mathcal{Y} \rightarrow [0, \infty)$ be the loss function comparing the output of f with the true outcome \mathcal{Y} . This describes a general multivariate regression case; in a probabilistic classification task with K classes we usually have $f : \mathcal{X} \rightarrow [0, 1]^K$. The risk function associated to our supervised learning task is $\mathcal{R}(f) := \mathbb{E}[\ell(f(x), y)]$. We cannot generally compute $\mathcal{R}(f)$, since the exact joint distribution $p(x, y)$ is unknown. However, an approximation of the risk can be obtained by computing the empirical risk by averaging the loss on the training sample. The objective is to minimize the target risk

¹The AUC is the area under the Receiver Operator Characteristic (ROC) curve, obtained by plotting classifier efficiency against the false positive rate for different classification thresholds (between $[0, 1]$).

$\mathcal{R}_T(f) := \mathbb{E}_{p_T(x,y)}[\ell(f(x), y)]$, via the labelled source data D_S and unlabelled target data D_T . Our task is to train a model function f that minimizes $\mathcal{R}_T(f)$, being able to compute only the source loss $\ell(f(x_S), y_S)$, but not the target loss $\ell(f(x_T), y_T)$. Section 2.2 reviews importance weighting methods to minimize the target risk under covariate shift.

2.2 Related Literature – Importance Weighting:

In an influential work, Shimodaira (2000) proposes a weighted maximum likelihood estimation (MWLE) and shows that this MWLE converges in probability to the minimizer of the target risk. Following Shimodaira (2000), assuming that the support of $p_T(x)$ is contained in $p_S(x)$, the expected loss (risk) w.r.t. \mathcal{D}_T equals that w.r.t. \mathcal{D}_S with weights $w(x) := p_T(x)/p_S(x)$ for the loss incurred by each x ,

$$\mathbb{E}_{\mathcal{D}_T} [\ell(f(x), y)] = \mathbb{E}_{\mathcal{D}_S} [w(x)\ell(f(x), y)] . \quad (1)$$

In short, the target risk can be minimized by weighting the source domain loss by a ratio of the densities of target and source domain features. The importance weights $w(x)$ are paramount in the covariate shift literature and several approaches optimize the estimation of the weights. One approach estimates the densities $p_T(x)$ and $p_S(x)$ separately (Shimodaira, 2000), e.g., through kernel density estimators (Sugiyama and Müller, 2005). Others estimate the density ratio directly, e.g., via Kernel-Mean-Matching (Huang et al., 2007), Kullback-Leibler importance estimation (KLIEP) (Sugiyama et al., 2008), and variations of unconstrained least-squares importance fitting (uLSIF) (Kanamori et al., 2009). Given $w(x)$, Sugiyama et al. (2007) propose importance weighted cross-validation (IWCV) and show that in theory this can deliver an almost unbiased estimate of the target risk. Zadrozny (2004) links covariate shift with selection bias, and shows that the target risk can be minimised by importance sampling of source domain data, employing the inverse probability of source set assignment for importance weights. This allows any probabilistic classifier to be used to obtain the weights, e.g., logistic regression (Bickel and Scheffer, 2007).

Although importance weighting in theory enables minimization of the target risk, there are challenges. Based on a measure of domain dissimilarity (e.g., Rényi divergence), Cortes et al. (2010) show that weighting leads to high generalization upper error bounds, making predictions unreliable, especially with large importance weights. In addition, Reddi et al. (2015) points out that while weighting can reduce bias, it can also greatly increase variance. Unfortunately, with increasing feature space dimension, the variance of the importance-weighted empirical risk estimates may increase sharply (Izbicki et al., 2014; Stojanov et al., 2019). This can be partly tackled by dimensionality reduction methods (Stojanov et al., 2019); see Kouw and Loog (2019) for a detailed discussion. We address these variance concerns via propensity scores.

2.3 Related Literature – Propensity scores in causal inference:

Given a set of observed covariates X and a binary indicator Z for treatment assignment (treatment vs control), RR83 introduce the propensity score as

$$e(X) := P(Z = 1|X) \quad (2)$$

and define treatment allocation Z as strongly ignorable, if

$$(i) \ (Y_1, Y_0) \perp\!\!\!\perp Z|X \quad \text{and} \quad (ii) \ 0 < e(X) < 1. \quad (3)$$

Condition (i) means that treatment assignment Z is conditionally independent of the potential outcome (Y_1, Y_0) , given the observed covariates. The potential outcomes are the possible outcomes for an object, depending on its treatment status, and at most one is observed, (e.g., for a treated object the observed outcome is $Y = Y_1$). In practice, condition (i) means that no confounders (covariates that are associated with the treatment and outcome) are unmeasured. RR83 show that if (3) holds, the propensity score is a balancing score. That is, given the propensity score, the distribution of the covariates in treatment and control are the same, i.e., $p(X|e(X), Z = 1) = p(X|e(x), Z = 0)$. Thus, conditional on the propensity score, unbiased average treatment effect estimates can be obtained, i.e., $\mathbb{E}[Y_1|e(x), Z = 1] - \mathbb{E}[Y_0|e(x), Z = 0] = \mathbb{E}[Y_1 - Y_0|e(x)]$. In practice, conditioning on the estimated (rather than true) propensity score can achieve better empirical balance as this corrects for statistical fluctuations in the sample as well (RR83; Hirano et al., 2003).

Below, we show how the propensity score methodology can be transferred to the covariate shift framework, for target risk minimization in supervised learning tasks.

3 A New Method: StratLearn

3.1 StratLearn – Methodology

In the covariate shift framework, we define the propensity score to be the probability that object i is in the source data, given its observed covariates, i.e.,

$$e(x_i) := P(s_i = 1|x_i), \text{ with } 0 < e(x_i) < 1. \quad (4)$$

Proposition 1 (Learning conditional on the propensity score). *If $p_S(x, y)$ and $p_T(x, y)$ satisfy the covariate shift definition and $0 < e(x) < 1$, then it holds that*

$$p_T(x, y|e(x)) = p_S(x, y|e(x)). \quad (5)$$

That is, conditional on $e(x)$ the joint source and target distributions are the same, eliminating covariate shift. It follows, for any loss function $\ell = \ell(f(x), y)$,

$$E_{p_T(x, y|e(x))}[\ell(f(x), y)] = E_{p_S(x, y|e(x))}[\ell(f(x), y)]. \quad (6)$$

Proposition 1 is verified in Section S1. Note that its condition, $0 < e(x) < 1$, is no stronger than the conditions required for (1). The support of $p_T(x)$ being contained in $p_S(x)$ implies $0 < e(x)$, and $e(x) = 1$ implies $p_T(x) = 0$, in which case the importance weight $w(x) = 0$, which is equivalent to discarding the sample.

With Proposition 1, we extend the basic causal inference theory to use propensity scores in the covariate shift framework. Conditioning on estimated propensity scores enables statistically principled minimization of the target risk based on source data. According to Proposition 1, if we were to condition on any single value of the propensity score, the distribution of x and y in the source and target domains would be identical and we could minimize their target risk using the source data alone. Because sample sizes with identical propensity scores are too small in practice for model fitting, we employ an approximation.

StratLearn takes advantage of Proposition 1 via propensity score stratification; source data D_S and target data D_T are divided into k non-overlapping subgroups (strata) based on quantiles of the estimated propensity scores. More precisely, letting q_j be the j 'th k -quantile of $\{e(x_i) : x_i \in (x_S \cup x_T)\}$, for $j \in 1, \dots, k$, we divide D_S and D_T into

$$D_{S_j}^{(k)} = \{(x, y) \in D_S : q_{k-j} < e(x) \leq q_{k-j+1}\} \text{ and } D_{T_j}^{(k)} = \{x \in D_T : q_{k-j} < e(x) \leq q_{k-j+1}\}, \quad (7)$$

where $q_0 = 0$ and $q_k = 1$. By Proposition 1, within strata,

$$p_{T_j}(y, x) \approx p_{S_j}(y, x), \text{ for } j \in 1, \dots, k, \quad (8)$$

where S_j indicates conditioning on assignment to the j 'th source stratum (analogously for target T_j). It follows that for $j \in 1, \dots, k$,

$$\mathbb{E}_{p_{T_j}(x, y)}[\ell(f(x), y)] \approx \mathbb{E}_{p_{S_j}(x, y)}[\ell(f(x), y)]. \quad (9)$$

Thus, we can minimize the target risk within strata by minimizing the source risk within strata. In this way, we reduce the covariate shift problem to non-overlapping subgroups where the source and target domain are approximately the same, which in principle allows us to fit any supervised learner to D_{S_j} to predict the target objects in D_{T_j} . Figure 1 presents a flow chart illustrating the steps of our proposed *StratLearn* methodology.

3.2 StratLearn – Technical Details

In general, any probabilistic classifier could be used to estimate propensity scores (e.g., Pirracchio et al. (2014)). Logistic regression is commonly used in causal inference, and we adopt it for the applications in this paper. In practice, the covariate shift assumption, $p_S(y|x) = p_T(y|x)$, requires there be no unobserved confounding covariates. To meet this requirement, we include all potential confounders as main effects. An estimate of the propensity scores in (4) is then obtained by probabilistic classification of source assignment, given source data x_S and target data x_T . Using the estimated propensity scores, the source and target data are grouped into strata, following (7).

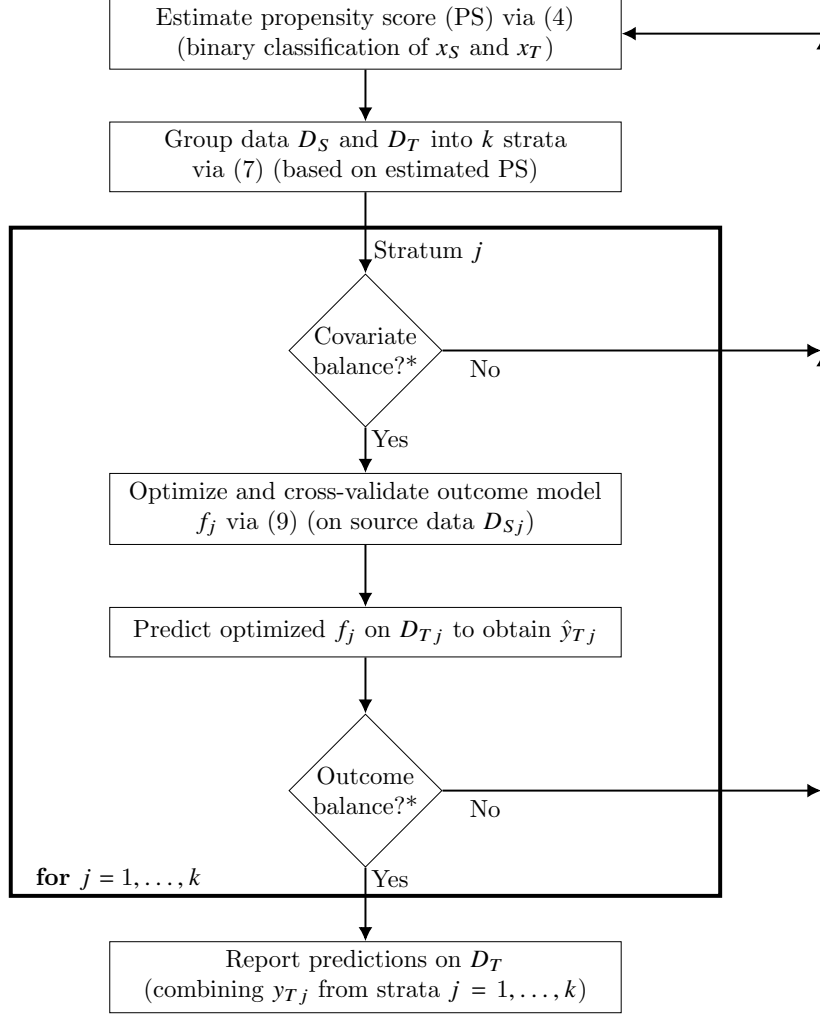


Fig. 1: *StratLearn* flow chart. (*Covariate balance and outcome balance is assessed as described in Section 3.3, with a numerical example given in Section 4.2.)

We use $k = 5$ strata based on empirical evidence provided by Cochran (1968), showing that sub-grouping into five strata is enough to remove at least 90% of the bias for many continuous distributions (RR83). Given the stratified data, we fit a model f_j to source data D_{Sj} , and predict the respective target samples in D_{Tj} , for $j \in 1, \dots, k$. Model hyperparameters for f_j can be selected through empirical risk minimization on source data D_{Sj} , for instance through cross-validation on D_{Sj} . The model functions f_j are trained independently and can be computed in parallel to reduce computational time. If the source distribution does not cover the target distribution well enough, some of the strata may contain too little source data to reliably train the model. In this case,

we add source data from one or more adjacent strata to avoid highly variable predictions. There is a bias-variance trade-off here in that this reduction in variance requires a relaxation of the approximation in (8), which inevitably increases bias somewhat. Although a general and precise criterion for combining the strata is elusive (more complex models require more data and data sets of the same size may be more or less informative for the same model), we illustrate the combination of source strata in Section 4.2 (and Section S7), where one or more source strata have insufficient data.

3.3 StratLearn – Balance Diagnostics

A key advantage of propensity scores derived in causal inference is their covariate balancing score property (RR83), that is, $p_S(x|e(x)) = p_T(x|e(x))$. In causal inference, this property is used to verify the propensity score model and/or the choice of covariates, x , e.g., by checking that x has the same within-strata distribution in the treatment and control groups. Employing the balancing property in the derivation of Proposition 1 allows us to take advantage of such diagnostic tools in our framework. We refer to the large literature on this (e.g., Rosenbaum and Rubin, 1984; Imai and van Dyk, 2004; Austin et al., 2007; Austin, 2011), and provide an example of such a balance check in Section 4.2 (and in Sections S6 and S7).

In Remark 1, we detail how additional structure in the covariate shift setting can be exploited to justify a corollary model diagnostic.

Remark 1. *In the propensity score framework of causal inference (Rosenbaum and Rubin, 1983) we have potential outcomes Y_0 and Y_1 . In the covariate shift framework, the potential outcomes are identical ($Y_0 \equiv Y_1$). That is, there is no “treatment effect” from being assigned to the source or target set, though only the source data are observed ($Y_1 \equiv Y$). Now, given the propensity score $e(x)$, with $0 < e(x) < 1$, and the covariate shift condition $p(y|x, s = 1) = p(y|x, s = 0)$, source data assignment is ‘strongly ignorable’ (using the terminology of RR83). It follows through Theorem 4 in RR83 that, conditional on the propensity score, source and target outcome are the same in expectation.*

In cases where labels are observed for (part of) the target group we can use Remark 1 as a model diagnostic. Although in practice the labels are mostly unobserved in the target group, they are available in our real-world scientific/experimental settings described in Sections 4.2 and 4.3. In Section 4.2 (as well as Sections S6, S7 and S8), we use Remark 1 to demonstrate a reduction of within-strata covariate shift (i.e., by conditioning on the propensity score).

We further demonstrate the possibility of similarly using predicted labels instead of actual labels as a model diagnostic. While the actual target labels y_T are usually not available in real-world data applications, the distribution of the model predicted outcome labels ($\tilde{y} = f(x)$) can be evaluated for source $f(x_S)$ and target $f(x_T)$. With f being a measurable function of the covariates x , and by employing the balancing property of propensity scores, it holds $p_S(f(x)|e(x)) = p_T(f(x)|e(x))$. Consequently, a discrepancy between the distributions of predicted source outcome $f(x_S)$ and predicted target outcome $f(x_T)$ is an indication of residual (covariate) shift in the source

and target distribution.² An advantage of assessing the balance in the predicted outcome $f(x)$ (in addition to covariate balance) is that $f(x)$ is designed to approximate the outcome y . Thus, a discrepancy of $f(x_S)$ and $f(x_T)$ indicates an imbalance in strongly predictive covariates, a straightforward sign for remaining, (likely) concerning confounding. We demonstrate the application of balance diagnostics via predicted labels in Section 4.2.

4 Numerical Demonstrations

4.1 Comparison Methods

We compare *StratLearn* to a range of well-established importance weighting methods.

- KLIEP – Kullback-Leibler importance estimation procedure (Sugiyama et al., 2008).
- uLSIF – Unconstrained least-squares importance fitting (Kanamori et al., 2009).³
- NN – Several versions of the nearest-neighbor importance weight estimator (Lima et al., 2008; Kremer et al., 2015; Loog, 2012), varying the number of neighbors.
- IPS – Importance weight estimation through probabilistic classification of source set assignment (Kanamori et al., 2009).

In Section 4.3, we incorporate the estimated weights as in the corresponding benchmark publication. Following Izbicki et al. (2017), the estimated weights are used for loss weighting as in (1). In Section 4.2, importance weighting has not previously been applied. We implement IWCV, importance sampling, and a combination of both, to demonstrate the advantage of *StratLearn* with respect to either; see Section S3.

4.2 Classification – SNIa Identification

Objective:

Type Ia supernovae (SNIa) are invaluable for the study of the accelerated expansion history of the universe (e.g., Riess et al., 1998; Perlmutter et al., 1999). SNIa are exploding stars that can be seen at large distances, occurring due to a particular physical scenario which causes their intrinsic luminosities to be (nearly) the same. This “standard candle” property of SNIa makes it possible to measure their distance, which in turn depends on parameters that describe the expansion of the universe.

To take advantage of this, reliable identification of SNIa based on photometric light curve (LC) data is a major challenge in modern observational cosmology. Photometric LC data are easily collectable, consisting of measurements of an astronomical object’s brightness (i.e. flux), filtered through different passbands (wavelength ranges), at a sequence of time points (as illustrated in Fig 2). Only a small subset of the objects are labelled via expensive spectroscopical observations. The labeled source data, D_S , are not representative of the photometric target data, D_T , as the selection of spectroscopic

²In practice, one has to ensure that f is not overfitted on the available training (source) data sample, a standard check in supervised learning, which can readily be assessed via standard validation tools, such as cross-validation or bootstrapping of source data.

³KLIEP and uLSIF were implemented with the original author’s public domain MATLAB code (link).

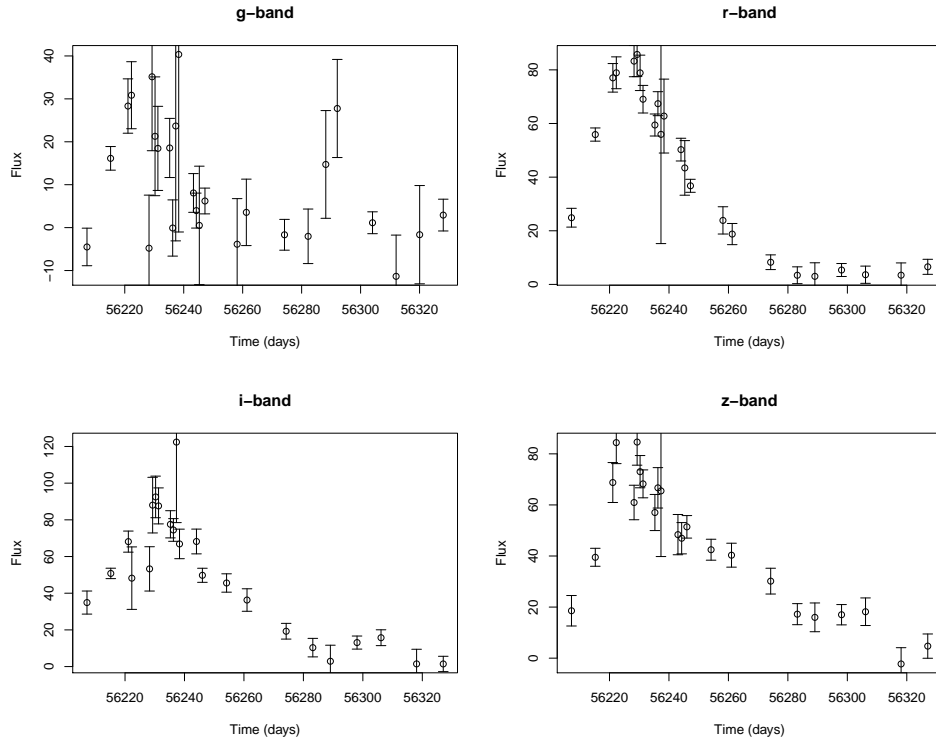


Fig. 2: Example of photometric LC data, including 1σ error bars, for a typical SNIa (specifically, SN2475 from the updated Kessler et al. (2010) simulated SPCC data).

source samples is biased towards brighter and bluer objects. The automatic classification of unlabelled objects, based on biased spectroscopically confirmed source data, is the subject of much research, including public classification challenges (Kessler et al., 2010, 2019).

Leading SNIa classification approaches are based on data augmentation; they sample synthetic objects from Gaussian process (GP) fits of the LCs to overcome covariate shift (Revsbech et al., 2018; Boone, 2019). The method of Revsbech et al. (2018) can be viewed as a prototype of *StratLearn*, as it augments the source data separately in strata based on the estimated propensity scores. However, to optimize data augmentation within strata, Revsbech et al. (2018) requires a sub-sample of labeled target data that is unavailable in practice. While effective in this particular case, GP data augmentation is not an option in most covariate shift tasks. We show that *StratLearn* makes augmentation unnecessary. We use target prediction AUC to compare performance to published results.

Data and Preprocessing:

We use data from the updated “Supernova photometric classification challenge” (SPCC) (Kessler et al., 2010), containing a total of 21,318 simulated SNIa and of other types (Ib, Ic and II). For each supernova (SN), LCs are given in four color bands, $\{g, r, i, z\}$. The data include a source set D_S of 1102 spectroscopically confirmed SNe with known types and 20,216 SNe with unknown types (target set D_T). 51% of the source objects are SNIa, while only 23% of the target data are SNIa, a consequence of the strong covariate shift in the data.

We follow the approach in Revsbech et al. (2018), which was applied to an earlier release of the SPCC data (Kessler et al., 2010, discussed in Section S6), to extract a set of features from the LC data that can be used for classification. First, a GP with a squared exponential kernel is used to model the LCs. Then, a diffusion map (Coifman and Lafon, 2006) (as used in Richards et al. (2012)) is applied, resulting in a vector of 100 similarity measures between the LCs that we use as predictor variables. Combining these with redshift (a measure of cosmological distance, defined in Section 4.3) and a measure of overall brightness, we obtain 102 predictive covariates.

Results:

To evaluate the impact of covariate shift on classification, we first consider a ‘biased fit’ by training a random forest classifier (as in Revsbech et al. (2018)) on the source covariates ignoring covariate shift, resulting in an AUC of 0.902 on the target data (black ROC curve in Fig 3). Next, we obtain a ‘gold standard’ benchmark by randomly selecting 1102 objects from target data as a representative source set. The same classification procedure with the unbiased ‘gold standard’ training data (unavailable in practice) yields an AUC of 0.972 on the remaining 19,114 target objects.

Given the biased source data, *StratLearn* is implemented as described in Section 3, including all 102 covariates in the logistic propensity score estimation model. After stratification, a random forest classifier is trained and optimized on source strata D_{S_1} and D_{S_2} separately to predict samples in target strata D_{T_1} and D_{T_2} . We use repeated 10-fold cross validation with a large hyperparameter grid to minimize the empirical risk of (9) within each strata, employing log-loss⁴ as our loss-function; details appear in Section S5. Source strata D_{S_j} for $j \in \{3, 4, 5\}$ have a small sample size, (13, 7, 4) respectively. Thus, source strata D_{S_j} for $j \in \{3, 4, 5\}$ are merged with D_{S_2} to train the random forest to predict D_{T_j} for $j \in \{3, 4, 5\}$. With *StratLearn*, we obtain an AUC of 0.958 on the target data (blue ROC curve in Fig 3), very near the optimal ‘gold standard’ benchmark.

Fig 3 compares *StratLearn* to importance sampling methods designed to adjust for covariate shift. For importance sampling, the bootstrapped samples in the random forest fit were resampled with probabilities proportional to the estimated importance weights (see Section S3). NN and IPS led to the best importance weighted classifier (AUC = 0.923, 0.921) – an improvement over the biased fit, but substantially lower than *StratLearn*. AUC standard errors (see Fig 3) are small relative to the large performance improvement of *StratLearn*. KLIEP failed to fit importance weights and is

⁴The log-loss (also referred to as cross-entropy loss) compares the output of a classification $f(x) \in [0, 1]$ with the true output y for an observation (x, y) via $\ell_{\text{logloss}}(f(x), y) := -(y \log(f(x)) + (1 - y) \log(1 - f(x)))$.

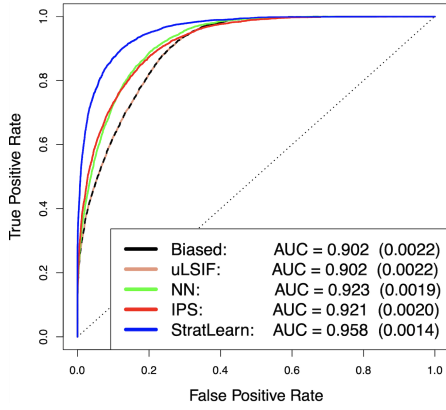


Fig. 3: Comparison of ROC curves for SNiA classification using the updated SPCC data. Here, Biased and uLSIF are identical. Bootstrap AUC standard errors (from 400 bootstrap samples) are given in parentheses.

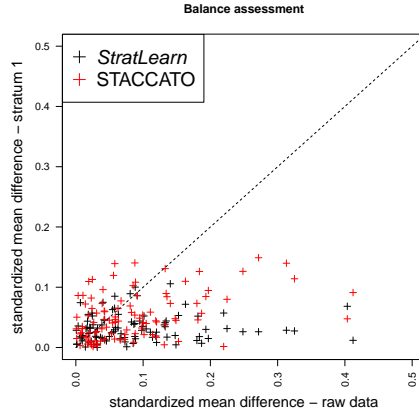


Fig. 4: Absolute standardized mean differences between source and target data of stratum 1 plotted against “raw” data absolute standardized mean differences for *StratLearn* and STACCATO.

thus not included in the results. We also implemented IWCV using the same hyperparameter grid as for *StratLearn*, and a combination of IWCV and importance sampling, which both led to lower AUC than the ones reported in Fig 3 (see Section S5).

Previous state-of-the-art methods report an AUC of 0.855 (Lochner et al., 2016) using boosted decision trees, 0.939 (Pasquet et al., 2019) using a framework of an autoencoder and a convolutional neural network and 0.94 (Revsbech et al., 2018) using LC augmentation and target data leakage, all lower than *StratLearn*.

Balance Assessment on updated SPCC data:

To illustrate the balancing property of propensity scores (see Section 3.3) and its effect on predictive target performance, we assess the covariate balance in the updated SPCC data within strata conditional on the estimated propensity scores, by means of two commonly used balance measures: absolute standardized mean differences (SMD) and the Kolmogorov-Smirnov test statistics (KS-stats) (Austin, 2011; Austin and Stuart, 2015).

Fig 4 provides a detailed covariate balance comparison, by plotting the “raw” SMD against the *StratLearn* SMD in stratum 1 (black) for each covariate. We remove two outliers (redshift and brightness) with very large “raw” SMD (1.1 and 1.7), because including them in the Figure makes it more difficult to illustrate the balance of the bulk of the covariates; both are well balanced in stratum 1 using *StratLearn* (SMD equals 0.12 and 0.17). Points below the diagonal line are better balanced in the stratum than in the “raw” non-stratified data. This is the case for the vast majority (71%) of black points in Fig 4, illustrating the balance improvement achieved with *StratLearn*.

Table 1: Strata composition on the updated SPCC data (Section 4.2), applying STACCATO (left) and *StratLearn* (right). The number of SNe, as well as the number and proportion of SNIa are presented in source and target stratum 1 and 2. For conciseness, we present the combined strata 3 to 5, containing too little source data for meaningful comparison of the SNIa proportions.

Stratum	Set	STACCATO			<i>StratLearn</i>		
		Number of SNe	Number of SNIa	Prop. of SNIa	Number of SNe	Number of SNIa	Prop. of SNIa
1	Source	924	414	0.45	958	518	0.54
	Target	3340	1125	0.34	3306	1790	0.54
2	Source	153	125	0.82	120	28	0.23
	Target	4111	973	0.24	4144	927	0.22
3 to 5	Source	25	19	0.76	24	12	0.5
	Target	12,765	2431	0.19	12,766	1812	0.14

Fig 4 also plots (red) the SMD achieved by STACCATO (Revsbech et al., 2018), which uses two covariates (redshift and brightness, as opposed to the 102 used by *StratLearn*) in the logistic regression to estimate propensity scores. While STACCATO improves the balance of the majority (69%) of the covariates, most (66%) black (*StratLearn*) SMD have smaller vertical values, indicating better balance than STACCATO (red).

On average across the 102 covariates, *StratLearn* improves covariate balance compared to the “raw” non-stratified data measured by SMD by $\sim 70\%$ in stratum 1 and $\sim 10\%$ in stratum 2 (KS-stats: $\sim 70\%$ in stratum 1 and $\sim 30\%$ in stratum 2)⁵. It further improves upon STACCATO by $\sim 36\%$ in stratum 1 and $\sim 46\%$ in stratum 2 using SMD (KS-stats: $\sim 24\%$ in stratum 1 and $\sim 36\%$ in stratum 2). The remaining strata contain too few source data to assess covariate balance. Details are provided in Table S2.

The improved covariate balance (reduced covariate shift) directly translates into improved predictive performance. STACCATO (including data augmentation and target data leakage) yields a target AUC of 0.94, whereas with *StratLearn* we obtain a target AUC of 0.958 (without data augmentation and no target data leakage) – a substantial improvement resulting from the improved covariate balance by accounting for potentially confounding covariates. In general, we note that balance is particularly important for covariates that are strongly predictive for the outcome. Domain-specific expertise might be necessary to identify such covariates in the individual cases in practice. In Section S7, we demonstrate how covariate balance can be improved by adjusting the propensity score model.

Table 1 presents the composition of the five *StratLearn* strata. Recall that according to Remark 1, conditional on the propensity score the marginal distributions of source and target outcome are the same in expectation. Table 1 shows that the proportion of SNIa in the source and target data (which in this case can be computed from knowledge of the true target labels in the simulation) align well for *StratLearn* in the first two strata, indicating the expected reduction in covariate shift. The source sample sizes in

⁵Percentages are calculated by taking the ratio of the average SMD (average KS-stats) of all 102 covariates.

Table 2: Outcome balance diagnostics via predicted labels on the updated SPCC data (Section 4.2), applying STACCATO (left) and *StratLearn* (right). The number and proportion of predicted SNIa are presented in source and target stratum 1 and 2. P-values are computed via Fisher’s exact test of independence between predicted SNIa target and source proportions within strata.

Stratum	Set	STACCATO (predicted)			<i>StratLearn</i> (predicted)		
		Number of SNIa	Prop. of SNIa	p-value	Number of SNIa	Prop. of SNIa	p-value
1	Source	414	0.45	8.4e-11	518	0.54	0.284
	Target	1106	0.33		1853	0.56	
2	Source	125	0.82	2.8e-13	28	0.23	0.749
	Target	2166	0.53		1040	0.25	

strata 3-5 are quite small, rendering meaningful comparison of the SNIa proportions impossible. In Strata 1 and 2, however, *StratLearn* achieves much better balance than either STACCATO or the raw (un-stratified) data (51% SNIa in source, 23% SNIa in target).

In Table 2, we demonstrate how predicted outcomes can be employed for balance diagnostics by assessing the predicted proportions of SNIa within strata obtained by STACCATO and by *StratLearn*. We compute the predicted outcomes by classifying objects to be SNIa if the (random forest) predicted SNIa probabilities are above 0.5. While STACCATO leads to a strong discrepancy between predicted SNIa proportions in the first two strata (indicating remaining confounding), *StratLearn* leads to well-matched predicted SNIa proportions. We further quantify the discrepancy by performing a two-sided Fisher’s exact test of independence, with the null hypothesis that there is no association of source/target set assignment and predicted SNIa proportion. Comparing different propensity score models, a higher p-value is an indicator for better balance in the predicted outcomes, and should thus be desirable. *StratLearn* leads to much higher p-values than STACCATO (failing to reject the null hypothesis for reasonable significance levels), which implies much weaker relation between source/target assignment and predicted outcomes.

In this particular example, with *StratLearn*, we fail to reject the null hypothesis for most significance levels. This may not always be the case (e.g., Section S6). We recall that the strategy of conditioning on propensity scores via stratification leads to subgroups with similar (not identical) propensity scores, and thus to similar (not identical) joint distributions within strata (this is the approximation in (8)). This in turn might lead to differences in the distributions of the covariates and the (predicted) outcomes, even if we could condition on the true propensity scores. We thus employ the p-values of (predicted) outcomes as an additional tool to assess, and primarily to compare, propensity score models to detect and reduce confounding of highly predictive and thus most relevant covariates.

4.3 Conditional Density Estimates – Photo- z Regression

Objective:

The wavelength of light from extragalactic objects is stretched because of the expansion of the universe – a phenomenon called ‘redshift’. This fractional shift towards the red end of the spectrum is denoted by z . A precise measurement of redshift allows cosmologists to estimate distances to astronomical sources, and its accurate quantification is essential for cosmological inference (e.g., redshift is a key component of the Big Bang theory). Because of instrumental limitations, redshift can be precisely measured only for a small fraction of the $\sim 10^7$ galaxies observed to date (set to grow to $\sim 10^9$ within a decade). These source data are subject to covariate shift relative to the set of galaxies with unknown redshift (target). Izbicki et al. (2017) employed importance weighting to adjust for covariate shift in x , a set of observed photometric magnitudes (a logarithmic measure of passband-filtered brightness), when estimating z . They obtain a non-parametric estimate of the full conditional density, $f(z|x)$, to quantify predictive uncertainty of redshift estimates. Proper quantification of predictive uncertainties is crucial to avoid systematic errors in the scientific downstream analysis (Izbicki et al., 2017; Sheldon et al., 2012). Using the same setup and conditional density estimation models (hist-NN, ker-NN, Series and Comb, detailed in Izbicki et al. (2017)),⁶ we show that *StratLearn* leads to better overall predictive performance than importance weighting.

Assuming that source and target data follow the same distribution, under the L^2 -loss, conditional density estimators typically aim to minimize the *generalized* risk (generalized in that the underlying loss can be negative):

$$\hat{R}(\hat{f}) = \frac{1}{n_S} \sum_{k=1}^{n_S} \int \hat{f}^2(z|x_S^{(k)}) dz - 2 \frac{1}{n_S} \sum_{k=1}^{n_S} \hat{f}(z_S^{(k)}|x_S^{(k)}), \quad (10)$$

Izbicki et al. (2017) propose to adjust for covariate shift by adapting (10), via optimizing weighted versions of the conditional density estimators (Izbicki et al., 2017, Sections 5.1-5.3) with respect to an importance weighted *generalized* risk:

$$\hat{R}_S(\hat{f}) = \frac{1}{n_T} \sum_{k=1}^{n_T} \int \hat{f}^2(z|x_T^{(k)}) dz - 2 \frac{1}{n_S} \sum_{k=1}^{n_S} \hat{f}(z_S^{(k)}|x_S^{(k)}) \hat{w}(x_S^{(k)}), \quad (11)$$

where the weights, $\hat{w}(x_S) = p_T(x)/p_S(x)$, are estimated using the methods described in Section 4.1. As their best performing model for $f(z|x)$, Izbicki et al. (2017) propose an average of importance weighted ker-NN and Series,

$$\hat{f}^\alpha(z|x) = \sum_{k=1}^p \alpha_k \hat{f}_k(z|x), \text{ with constraints (i): } \alpha_i \geq 0, \text{ and (ii): } \sum_{k=1}^p \alpha_k = 1, \quad (12)$$

⁶For the computation of the conditional density estimators we used code by Izbicki et al. (2017) (link).

referred to as ‘Comb’ (i.e., combination), where $p = 2$ and α_i is optimized to minimize (11).

With *StratLearn*, we optimize the unweighted conditional density estimators (hist-NN, ker-NN, Series) by minimizing (10) in each source stratum separately (accounting for covariate shift following Proposition 1). We also propose a *StratLearn* version of Comb by optimizing (12) on each source stratum separately (via the generalized risk in (11) with $w(x) \equiv 1$), including ker-NN and Series (each optimized via *StratLearn* beforehand). *StratLearn* and the other methods are compared with a ‘Biased’ (unweighted) method that simply optimizes (10). We abbreviate the combination of each method (*StratLearn*, ‘Biased’, and each of the weighting methods in Section 4.1) with the models for $f(z|x)$ (hist-NN, ker-NN, Series and Comb) as $\text{Method}_{\text{Model}}$.

Data:

We use the same data as Izbicki et al. (2017), consisting of 467,710 galaxies from Sheldon et al. (2012), each with spectroscopic redshift z (measured with negligible error), and five photometric covariates x . As in Izbicki et al. (2017), we use the r-band magnitude and the four colors (differences of magnitude values in adjacent photometric bands) as our covariates. We denote this spectroscopic source sample by D_S . To simulate realistic covariate shift, we follow Izbicki et al. (2017): starting from D_S , we use rejection sampling to simulate a photometric, unrepresentative target sample D_T , with the prescription $p(s = 0|x) = f_{B(13,4)}(x_{(r)})/\max_{x_{(r)}} f_{B(13,4)}(x_{(r)})$, where $x_{(r)}$ is the r-band magnitude and $f_{B(13,4)}$ is a beta density with parameters (13,4). Additionally, we investigated adding $k \in \{10, 50\}$ i.i.d. standard normal covariates as potential predictors to the 5 photometric covariates. This simulates the realistic case where additional potentially confounding covariates are present. For comparability, we follow Izbicki et al. (2017) and use $|D_S^{\text{train}}| = 2800$ galaxies randomly sampled from D_S as training data, plus a validation set of $|D_S^{\text{val}}| = 1200$ galaxies. We assess the performance of each $\text{Method}_{\text{Model}}$ pair using a random subset of D_T , i.e., $|D_T^{\text{test}}| = 6000$.

Results:

For evaluation of \hat{f} under each $\text{Method}_{\text{Model}}$ pair, we use the (in our simulation) known target redshifts, z_T , to compute the target risk, $\hat{R}_T(\hat{f})$, via a non-weighted version of (11) with $x_S^{(k)}$ and $y_S^{(k)}$ replaced by $x_T^{(k)}$ and $y_T^{(k)}$, given by:

$$\hat{R}_T(\hat{f}) = \frac{1}{n_T} \sum_{k=1}^{n_T} \int \hat{f}^2(z|x_T^{(k)}) dz - 2 \frac{1}{n_T} \sum_{k=1}^{n_T} \hat{f}(z_T^{(k)}|x_T^{(k)}). \quad (13)$$

Fig 5 compares the resulting target risk \hat{R}_T across models and covariate sets, showing that *StratLearn_{Comb}* gives the best performance in all three covariate setups.

For small covariate space dimension (Fig 5, left panel), *StratLearn_{Comb}* improves upon *StratLearn_{ker-NN}* and *StratLearn_{Series}*, optimizing the source risk in each stratum separately and combining their predictions. In the presence of potential additional confounding covariates (Fig 5, middle and right panels), the performance of the Series

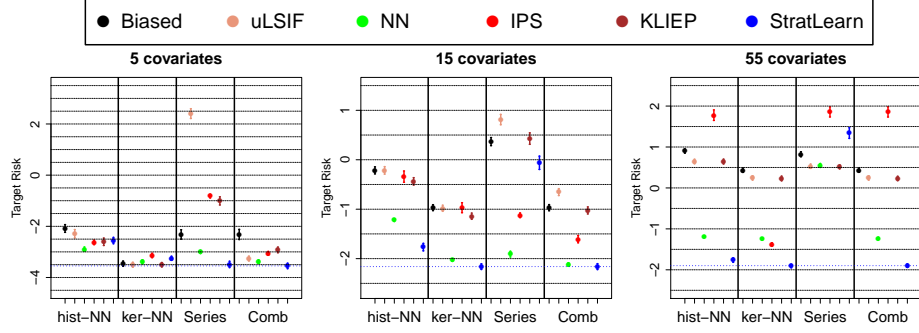


Fig. 5: Target risk (\hat{R}_T) of the four photo- z estimation models under each method (different colors), using different sets of predictors. Bars give the mean ± 2 bootstrap standard errors (from 400 bootstrap samples).

estimator degrades strongly under most methods. In these cases, $StratLearn_{Comb}$ exploits the higher performance of $StratLearn_{ker-NN}$. In contrast, for the non-adjusted (Biased) and importance weighted methods (e.g. IPS), the combination of approaches (Comb) does not necessarily lead to improved performance (e.g., $IPSComb$ exhibits a higher target risk than $IPScer-NN$ on its own (Fig 5, right panel)), indicating that the optimization in (12) fails due to remaining covariate shift in the data. More precisely, the weighted empirical *source* risk minimization ((11), as a form of (1)) does not lead to *target* risk minimization in these situations. In general, the improvement of $StratLearn$ relative to weighting methods increases with the dimensionality of the covariate space, leading to a more robust regime.

5 Discussion

We provide a simple, though statistically principled and theoretically justified method for learning under covariate shift conditions. We show that $StratLearn$ outperforms a range of state-of-the-art importance weighting methods on two contemporary research questions in cosmology (and on toy covariate shift examples, Section S7), especially in the presence of a high-dimensional covariate space. The assumption of covariate shift is rather strong, requiring that there are no unmeasured confounding covariates – something that cannot be guaranteed in general. In Section S7, however, we demonstrate a certain robustness of our method against violation of this assumption. Further work is necessary to assess more fully the performance of $StratLearn$ when this assumption is only approximately fulfilled. We emphasize that the covariate shift framework is best justified in the presence of a large number of covariates mitigating the risk of unmeasured confounders – in which case it is critical to adopt a method that, like $StratLearn$, can robustly handle many covariates. Our framework is entirely general and versatile, as illustrated with examples of regression, conditional density estimation and classification. Notably, our numerical demonstrations illustrate the advantage of using only a subset of the source data when formulating predictions for individual objects in

the target, where the subset is chosen for its similarity to the target data in question (through stratification). This is a markedly different strategy to the widespread practice of including all possible available observations when fitting learning models.

The novelty of our approach is grounded in the transfer of the well-established causal inference propensity score framework (RR83) to the domain adaptation/covariate shift setting, by demonstrating that a method established to obtain unbiased treatment effect estimates can be adapted to optimize the target risk of a supervised learner under covariate shift. In future work, this extension gives a chance to transfer hard won practical advice from causal inference (e.g., balance diagnostics, estimation of propensity scores, choice of included covariates (Rosenbaum and Rubin, 1984; Austin et al., 2007; Pirracchio et al., 2014), etc.) to the covariate shift framework. We will also explore the possibility of taking advantage of Proposition 1 through a matching approach (Imbens and Rubin, 2015), which could prove more sensitive to the underlying propensity score distribution. We believe *StratLearn* may become a powerful alternative to importance weighting, with a myriad of possible extensions and applications.

6 Acknowledgements:

David van Dyk acknowledges partial support from the UK Engineering and Physical Sciences Research Council [EP/W015080/1]; Roberto Trotta’s work was partially supported by STFC in the UK [ST/P000762/1, ST/T000791/1]; and David Stenning acknowledges the support of the Natural Sciences and Engineering Research Council of Canada (NSERC) [RGPIN-2021-03985]. Finally, van Dyk, Stenning and Autenrieth acknowledge support from the Marie-Skłodowska-Curie RISE [H2020-MSCA-RISE-2019-873089] Grant provided by the European Commission. *The authors report there are no competing interests to declare.*

References

- Austin, P.C. 2011. An introduction to propensity score methods for reducing the effects of confounding in observational studies. *Multivariate behavioral research* 46(3): 399–424 .
- Austin, P.C., P. Grootendorst, and G.M. Anderson. 2007. A comparison of the ability of different propensity score models to balance measured variables between treated and untreated subjects: a monte carlo study. *Statistics in medicine* 26(4): 734–753 .
- Austin, P.C. and E.A. Stuart. 2015. Moving towards best practice when using inverse probability of treatment weighting (iptw) using the propensity score to estimate causal treatment effects in observational studies. *Statistics in medicine* 34(28): 3661–3679 .
- Austin, P.C. and E.A. Stuart. 2017. The performance of inverse probability of treatment weighting and full matching on the propensity score in the presence of model

- misspecification when estimating the effect of treatment on survival outcomes. *Statistical methods in medical research* 26(4): 1654–1670 .
- Bickel, S. and T. Scheffer 2007. Dirichlet-enhanced spam filtering based on biased samples. In *Advances in neural information processing systems*, pp. 161–168.
- Boone, K. 2019. Avocado: Photometric classification of astronomical transients with gaussian process augmentation. *The Astronomical Journal* 158(6): 257 .
- Calders, T., A. Karim, F. Kamiran, W. Ali, and X. Zhang 2013. Controlling attribute effect in linear regression. In *2013 IEEE 13th international conference on data mining*, pp. 71–80. IEEE.
- Chan, A., A. Alaa, Z. Qian, and M. Van Der Schaar 2020. Unlabelled data improves bayesian uncertainty calibration under covariate shift. In *International Conference on Machine Learning*, pp. 1392–1402. PMLR.
- Cochran, W.G. 1968. The effectiveness of adjustment by subclassification in removing bias in observational studies. *Biometrics*: 295–313 .
- Coifman, R.R. and S. Lafon. 2006. Diffusion maps. *Applied and computational harmonic analysis* 21(1): 5–30 .
- Cortes, C., Y. Mansour, and M. Mohri 2010. Learning bounds for importance weighting. In *Advances in neural information processing systems*, pp. 442–450.
- Dua, D. and C. Graff. 2017. UCI machine learning repository.
- Heckman, J.J. 1979. Sample selection bias as a specification error. *Econometrica: Journal of the econometric society*: 153–161 .
- Hirano, K., G.W. Imbens, and G. Ridder. 2003. Efficient estimation of average treatment effects using the estimated propensity score. *Econometrica* 71(4): 1161–1189 .
- Huang, J., A. Gretton, K. Borgwardt, B. Schölkopf, and A.J. Smola 2007. Correcting sample selection bias by unlabeled data. In *Advances in neural information processing systems*, pp. 601–608.
- Imai, K. and D.A. van Dyk. 2004. Causal inference with general treatment regimes: Generalizing the propensity score. *Journal of the American Statistical Association* 99(467): 854–866 .
- Imbens, G.W. and D.B. Rubin. 2015. *Causal inference in statistics, social, and biomedical sciences*. Cambridge University Press.
- Izbicki, R., A. Lee, and C. Schafer 2014. High-dimensional density ratio estimation with extensions to approximate likelihood computation. In *Artificial Intelligence*

- and *Statistics*, pp. 420–429. PMLR.
- Izbicki, R., A.B. Lee, P.E. Freeman, et al. 2017. Photo- z estimation: An example of nonparametric conditional density estimation under selection bias. *The Annals of Applied Statistics* 11(2): 698–724 .
- Kanamori, T., S. Hido, and M. Sugiyama. 2009. A least-squares approach to direct importance estimation. *Journal of Machine Learning Research* 10(Jul): 1391–1445 .
- Kessler, R., B. Bassett, P. Belov, V. Bhatnagar, H. Campbell, A. Conley, J.A. Frieman, A. Glazov, S. González-Gaitán, R. Hlozek, et al. 2010. Results from the supernova photometric classification challenge. *Publications of the Astronomical Society of the Pacific* 122(898): 1415 .
- Kessler, R., A. Conley, S. Jha, and S. Kuhlmann. 2010. Supernova photometric classification challenge. *arXiv preprint arXiv:1001.5210* .
- Kessler, R., G. Narayan, A. Avelino, E. Bachelet, R. Biswas, P. Brown, D. Chernoff, A. Connolly, M. Dai, S. Daniel, et al. 2019. Models and simulations for the photometric lsst astronomical time series classification challenge (plasticc). *Publications of the Astronomical Society of the Pacific* 131(1003): 094501 .
- Kouw, W.M. and M. Loog. 2019. A review of domain adaptation without target labels. *IEEE transactions on pattern analysis and machine intelligence* .
- Kremer, J., F. Gieseke, K.S. Pedersen, and C. Igel. 2015. Nearest neighbor density ratio estimation for large-scale applications in astronomy. *Astronomy and Computing* 12: 67–72 .
- Lima, M., C.E. Cunha, H. Oyaizu, J. Frieman, H. Lin, and E.S. Sheldon. 2008. Estimating the redshift distribution of photometric galaxy samples. *Monthly Notices of the Royal Astronomical Society* 390(1): 118–130 .
- Little, R.J. and D.B. Rubin. 2019. *Statistical analysis with missing data*, Volume 793. John Wiley & Sons.
- Liu, A. and B.D. Ziebart 2014. Robust classification under sample selection bias. In *NIPS*, pp. 37–45.
- Lochner, M., J.D. McEwen, H.V. Peiris, O. Lahav, and M.K. Winter. 2016. Photometric supernova classification with machine learning. *The Astrophysical Journal Supplement Series* 225(2): 31 .
- Loog, M. 2012. Nearest neighbor-based importance weighting. In *2012 IEEE International Workshop on Machine Learning for Signal Processing*, pp. 1–6. IEEE.
- Lunceford, J.K. and M. Davidian. 2004. Stratification and weighting via the propensity score in estimation of causal treatment effects: a comparative study. *Statistics in*

medicine 23(19): 2937–2960 .

- Magliacane, S., T. van Ommen, T. Claassen, S. Bongers, P. Versteeg, and J.M. Mooij. 2018. Domain adaptation by using causal inference to predict invariant conditional distributions. In *Advances in Neural Information Processing Systems*, pp. 10846–10856.
- Moreno-Torres, J.G., T. Raeder, R. Alaiz-Rodríguez, N.V. Chawla, and F. Herrera. 2012. A unifying view on dataset shift in classification. *Pattern Recognition* 45(1): 521–530 .
- Pan, S.J., I.W. Tsang, J.T. Kwok, and Q. Yang. 2010. Domain adaptation via transfer component analysis. *IEEE Transactions on Neural Networks* 22(2): 199–210 .
- Pan, S.J. and Q. Yang. 2009. A survey on transfer learning. *IEEE Transactions on knowledge and data engineering* 22(10): 1345–1359 .
- Pasquet, J., J. Pasquet, M. Chaumont, and D. Fouchez. 2019. Pelican: deep architecture for the light curve analysis. *Astronomy & Astrophysics* 627: A21 .
- Perlmutter, S., G. Aldering, G. Goldhaber, R. Knop, P. Nugent, P. Castro, S. Deustua, S. Fabbro, A. Goobar, D. Groom, et al. 1999. Measurements of ω and λ from 42 high-redshift supernovae. *The Astrophysical Journal* 517(2): 565 .
- Pirracchio, R., M.L. Petersen, and M. van der Laan. 2014. Improving propensity score estimators’ robustness to model misspecification using super learner. *American journal of epidemiology* 181(2): 108–119 .
- Reddi, S., B. Póczos, and A. Smola. 2015. Doubly robust covariate shift correction. In *Proceedings of the AAAI Conference on Artificial Intelligence*, Volume 29.
- Revsbech, E.A., R. Trotta, and D.A. van Dyk. 2018. Staccato: a novel solution to supernova photometric classification with biased training sets. *Monthly Notices of the Royal Astronomical Society* 473(3): 3969–3986 .
- Richards, J.W., D. Homrighausen, P.E. Freeman, C.M. Schafer, and D. Poznanski. 2012. Semi-supervised learning for photometric supernova classification. *Monthly Notices of the Royal Astronomical Society* 419(2): 1121–1135 .
- Riess, A.G., A.V. Filippenko, P. Challis, A. Clocchiatti, A. Diercks, P.M. Garnavich, R.L. Gilliland, C.J. Hogan, S. Jha, R.P. Kirshner, et al. 1998. Observational evidence from supernovae for an accelerating universe and a cosmological constant. *The Astronomical Journal* 116(3): 1009 .
- Rivera, W.A., A. Goel, and J.P. Kincaid. 2014. Oups: a combined approach using smote and propensity score matching. In *2014 13th International Conference on Machine Learning and Applications*, pp. 424–427. IEEE.

- Rosenbaum, P.R. and D.B. Rubin. 1983. The central role of the propensity score in observational studies for causal effects. *Biometrika* 70(1): 41–55 .
- Rosenbaum, P.R. and D.B. Rubin. 1984. Reducing bias in observational studies using subclassification on the propensity score. *Journal of the American statistical Association* 79(387): 516–524 .
- Rubin, D.B. 2004. On principles for modeling propensity scores in medical research. *Pharmacoepidemiology and drug safety* 13(12): 855–857 .
- Sheldon, E.S., C.E. Cunha, R. Mandelbaum, J. Brinkmann, and B.A. Weaver. 2012. Photometric redshift probability distributions for galaxies in the sdss dr8. *The Astrophysical Journal Supplement Series* 201(2): 32 .
- Shimodaira, H. 2000. Improving predictive inference under covariate shift by weighting the log-likelihood function. *Journal of statistical planning and inference* 90(2): 227–244 .
- Stojanov, P., M. Gong, J. Carbonell, and K. Zhang 2019. Low-dimensional density ratio estimation for covariate shift correction. In *The 22nd International Conference on Artificial Intelligence and Statistics*, pp. 3449–3458. PMLR.
- Sugiyama, M., M. Krauledat, and K.R. Müller. 2007. Covariate shift adaptation by importance weighted cross validation. *Journal of Machine Learning Research* 8(May): 985–1005 .
- Sugiyama, M. and K.R. Müller. 2005. Input-dependent estimation of generalization error under covariate shift. *Statistics & Risk Modeling* 23(4): 249–279 .
- Sugiyama, M., S. Nakajima, H. Kashima, P.V. Buenau, and M. Kawanabe 2008. Direct importance estimation with model selection and its application to covariate shift adaptation. In *Advances in neural information processing systems*, pp. 1433–1440.
- Zadrozny, B. 2004. Learning and evaluating classifiers under sample selection bias. In *Proceedings of the twenty-first international conference on Machine learning*, pp. 114. ACM.

Supplemental Materials

S1 Additional Methodological Details for *StratLearn*

In this section, we provide additional information for our novel *StratLearn* methodology described in Section 3, by formally deriving Proposition 1.

Verification of Proposition 1: For Proposition 1, we start from [Theorem 1] in Rosenbaum and Rubin (1983), which proves that the propensity score $e(x)$, with $0 < e(x) < 1$, is a balancing score, which for our case means

$$x \perp\!\!\!\perp s | e(x), \quad (14)$$

or equivalently $p_S(x|e(x)) = p_T(x|e(x))$. That is, conditional on the propensity score, the covariates in the source and target data have the same distribution. It follows that

$$\begin{aligned} p_S(x, y|e(x)) &:= p(x, y|e(x), s = 1) \\ &= p(y|x, e(x), s = 1)p(x|e(x), s = 1) \end{aligned} \quad (15)$$

$$= p(y|x, e(x), s = 0)p(x|e(x), s = 1) \quad (16)$$

$$= p(y|x, e(x), s = 0)p(x|e(x), s = 0) \quad (17)$$

$$= p(x, y|e(x), s = 0)$$

$$=: p_T(x, y|e(x)).$$

Step (16) follows from the covariate shift assumption that $p(y|x, s = 1) = p(y|x, s = 0)$, with $e(x)$ as a function of x not changing the conditional distributions. Step (17) follows from the balancing property of the propensity score (14). Thus, conditional on the propensity score, the source and target data have the same joint distribution. Equation (6) follows directly.

S2 Bibliographic Note

In this section, we provide additional background literature to supplement examples provided in the main paper.

The purpose of domain adaptation methods is to obtain accurate target (test) predictions in situations where the source data domain is not an accurate representation of the target data domain. Quionero-Candela et al. (2009) provide a comprehensive overview of such domain shift, or “dataset shift”, in machine learning. Domain adaptation cases arise in a myriad of applications, such as in medical imaging (Stonnington et al., 2008; Van Oopbroek et al., 2014; Kamnitsas et al., 2017), where mechanical configurations may vary between medical centers; natural language processing (Jiang and Zhai, 2007), where annotated source data is often highly specialized and thus different from the target data; robotics and computer vision (Patel et al., 2015; Hoffman et al., 2016; Tai et al., 2017; Csurka, 2017), where simulated and observed data is combined to improve classification performance on the unlabeled target data; and astronomy

(Gieseke et al., 2010; Vilalta et al., 2013; Freeman et al., 2017; Revsbech et al., 2018; Allam Jr et al., 2018; Möller and de Boissière, 2020), where brighter astronomical objects are more likely to be observed and therefore included in the source set.

With increasing interest in the learning community, a variety of methods have been proposed, which (following Kouw and Loog (2019)) can be mainly organized in three categories: feature based methods, such as subspace mappings (Fernando et al., 2013; Gong et al., 2013; Kouw et al., 2016), finding domain-invariant spaces (Pan et al., 2010; Gong et al., 2016) and optimal transport (Courty et al., 2016, 2017); inference based methods, including minimax estimators (Liu and Ziebart, 2014; Wen et al., 2014; Chen et al., 2016) and self-learning (Bruzzone and Marconcini, 2009; Yoon et al., 2020); and, thirdly, sample based approaches, with a focus on importance weighting (Shimodaira, 2000; Sugiyama et al., 2008; Cortes et al., 2010; Bickel et al., 2009), mainly in the covariate shift framework.

The estimation of importance weights is central in the covariate shift framework, with a variety of different approaches. Yu and Szepesvári (2012) and Baktashmotlagh et al. (2014) estimate the densities separately, e.g. through kernel density estimators. Based on Huang et al. (2007), Wen et al. (2015) propose Kernel-Mean-Matching in a reproducing kernel Hilbert space employing the frank-wolfe algorithm. Kanamori et al. (2012) describe variations of unconstrained least-squares importance fitting (uLSIF) (Kanamori et al., 2009). Tsuboi et al. (2009) propose a variation of KLIEP (Sugiyama et al., 2008), adopting a log-linear function to model the importance weights. To alleviate the poor performance issue of weighting in high-dimensional covariate spaces, Sugiyama et al. (2010) and Sugiyama et al. (2011) propose the incorporation of dimensionality reduction procedures when estimating density ratios. In theoretical work, Ben-David et al. (2007) and Ben-David et al. (2010) derive generalization bounds, and conditions under which a classifier can learn from source data to perform well on target data. Cortes et al. (2008) theoretically analyze the effect of errors in the weight estimation on the outcome hypothesis of the learning algorithm. More recently, there have been efforts to transfer methods between the causal inference and domain adaptation framework (Rojas-Carulla et al., 2018; Magliacane et al., 2018; Hassanpour and Greiner, 2019).

In the causal inference framework, the introduction of propensity scores (Rosenbaum and Rubin, 1983) has been groundbreaking. There has been vast work on generalization, best-practice, and assessment of propensity scores in causal inference (e.g., Hirano et al., 2003; Imai and van Dyk, 2004; Lunceford and Davidian, 2004; Stuart et al., 2013; Franklin et al., 2014; Austin and Stuart, 2015; Griffin et al., 2017). While the general methodology has not yet been considered in the domain adaptation framework, it has been transferred to other areas, such as learning from positive and unlabeled data (Bekker et al., 2019), unbiased learning-to-rank (Joachims et al., 2017), or the evaluation of recommender systems (Schnabel et al., 2016), supplementing the examples provided in Section 1. Much work has been done to improve propensity score estimators to obtain unbiased treatment effects, with various proposed methods (e.g., McCaffrey et al., 2004; Setoguchi et al., 2008; Lee et al., 2010; Westreich et al., 2011; McCaffrey et al., 2013; Pirracchio et al., 2014; Imai and Ratkovic, 2014; Pirracchio and Carone, 2018; Autenrieth et al., 2021). In the examples provided in the main paper,

we show that *StratLearn* with a simple logistic regression propensity score estimator leads to strong predictive target performance, outperforming various importance weighting methods. The consideration of additional propensity score estimators, as well as optimizing the set of selected covariates, might further improve *StratLearn* in future work, e.g. by directly targeting covariate balance, similar to (Griffin et al., 2017; Parast et al., 2017; Pirracchio and Carone, 2018).

We note that the additional literature described in this section is by far not complete, but rather serves as an additional overview of the domain adaptation/covariate shift framework, and allows further placement of our work within this framework. We refer to surveys provided in the literature for a more thorough discussion on the topic (Pan and Yang, 2009; Kouw and Loog, 2019). The summary of propensity score methods serves as an overview of the extensive work that can potentially be transferred from causal inference to the covariate shift framework, by transferring the general propensity score methodology as described in Section 3. We refer to Imbens and Rubin (2015) for a more comprehensive summary on propensity scores.

S3 Details of Comparison Models

Here we detail our implementation of the several methods listed in Section 4.1 that we compare with *StratLearn* in our numerical studies.

Importance Weighting Estimators:

Following Kanamori et al. (2009) and Bickel et al. (2009), by Bayes Theorem,

$$w(x) = \frac{p_T(x)}{p_S(x)} = \frac{p(s=1)}{p(s=0)} \frac{p(s=0|x)}{p(s=1|x)} \approx \frac{n_S}{n_T} \left(\frac{1}{p(s=1|x)} - 1 \right). \quad (18)$$

The importance-weighting-based estimators, KLIEP, uLSIF and NN (described in Section 4.1) directly estimate $w(x)$. IPS obtains an estimate of $w(x)$ by plugging in the estimated propensity score into the right-hand side of (18), which allows any probabilistic classifier to be used to obtain the weights, e.g., logistic regression (Bickel and Scheffer, 2007). The estimated weights in (18) can then be used for weighted empirical risk minimization (following Formula (1)); e.g., through (11) in Section 4.3, and through IWCV in Section 4.2.

To implement importance sampling, such as in Section 4.2, we employ the framework proposed by Zadrozny (2004). Specifically, Zadrozny (2004) shows that for any distribution \mathcal{D} with feature-label-selection space $\mathcal{X} \times \mathcal{Y} \times \mathcal{S}$ and (x, y, s) examples drawn from \mathcal{D} , for all classifiers f and loss functions $\ell = \ell(f(x), y)$, if we assume that $P(s=1|x, y) = P(s=1|x) \neq 0$, then

$$\mathbb{E}_{\mathcal{D}} [\ell(f(x), y)] = \mathbb{E}_{\hat{\mathcal{D}}} [\ell(f(x), y) | s = 1], \quad (19)$$

$$\text{with } \hat{\mathcal{D}}(x, y, s) := \frac{P(s=1)}{P(s=1|x)} \mathcal{D}(x, y, s). \quad (20)$$

The target risk can thus be minimised by sampling from $\hat{\mathcal{D}}$, e.g., by importance sampling of source domain data. Formula (20) allows us to directly use the inverse of the estimated propensity scores. Moreover, rearranging the terms in the formulation of $w(x)$ in the right hand side of (18) yields

$$p(s=0)w(x) + p(s=1) = \frac{p(s=1)}{p(s=1|x)}. \quad (21)$$

Then, substituting into (20),

$$\hat{\mathcal{D}}(x, y, s) := \frac{P(s=1)}{P(s=1|x)} \mathcal{D}(x, y, s) \quad (22)$$

$$= (w(x)p(s=0) + p(s=1)) \mathcal{D}(x, y, s). \quad (23)$$

Thus, following Formula (19) (Zadrozny, 2004), IPS can be used for importance sampling via (22), and the direct-weight estimators KLIEP, uLSIF and NN can be used for importance sampling via (23).

S4 Details of Data and Software

The data required to reproduce the results for supernova classification, as presented in Section 4.2 of the main paper, and Sections S5 and S6 of this Supplement, can be found here: [SPCC data link](#). The data used for photometric redshift regression, as presented in Section 4.3 was used by permission of the original authors of Sheldon et al. (2012). The data used from the UCI repository (Dua and Graff, 2017) is publicly available ([UCI Wine quality data link](#)), [Parkinsons Telemonitoring Data link](#))).

The *StratLearn* software that we provide is written in R (R Core Team, 2019). For computation of the experiments, a 32 CPU Core cluster was available to speed up the simulations. However, computation time/resources was not a significant issue for the numerical results in this paper. As a benchmark, using a MacBook Pro with a 2.3 GHz 8-Core i9 processor, one scenario (e.g., medium covariate shift, high-dimensional covariate set) for conditional density estimation on SDSS data took less than 8 hours to run. All other experiments are less time-consuming. The supernova classification (Section 4.2) on preprocessed SPCC data (provided in the link above) took less than 2 hours on the same MacBook Pro.

S5 Additional Results for SNIa Identification

This Section provides additional results and details complementing Section 4.2, which describes the classification of supernovae (SNe) into type 1a (SNIa) and non-SNIa based on photometric light curve data, given a strongly biased source data set from Kessler et al. (2010).

Random Forest Implementation and Hyperparameter Selection:

We use the “ranger” random forest implementation in **caret** (Kuhn, 2008) for SNe classification in this paper. Repeated 10-fold cross-validation (with five repetitions)

Table S1: AUC results on the updated SPCC (photometric) target data (Kessler et al., 2010), using various importance weighting approaches to adjust for covariate shift.

	IWCV	importance sampling	IWCV + importance sampling
uLSIF	0.906	0.902	0.906
NN	0.897	0.923	0.914
IPS	0.897	0.921	0.924

is implemented with a large hyperparameter grid, containing four different numbers of covariates to possibly split at in each node (3,5,8,10); five values for minimum node size (3,5,7,10,20); and two different splitting rules (“gini” and “extratrees”). To optimize the selected hyperparameter setting, we compute the average log-loss via cross-validation on source data. Using *StratLearn*, cross-validation for hyperparameter selection (optimizing the average log-loss) is done on each source group separately (with groups defined in Section 4.2). We employ the log-loss to compute the empirical risk by evaluating the loss function $l(f(x), y)$ on each sample separately as described in Section 2. The AUC (used to assess target predictive performance in this example) does not include the evaluation of a loss function that compares the true label y and prediction $f(x)$ for each sample x separately. However, to demonstrate robustness w.r.t. the choice of hyperparameter optimization, we also compute the AUC on source data (on each source group separately) via cross-validation, which leads to the same hyperparameter setting as using the log-loss.

Comparison of Importance Weighting Methods:

In addition to importance sampling (as presented in Figure 3), we investigate two further importance weighting approaches to obtain a comprehensive performance comparison of importance weighting and *StratLearn*. More precisely, we implement IWCV, and a combination of IWCV and importance sampling. Table S1 presents the resulting target AUC for all implemented weighting methods. In summary, none of the importance weighting methods are competitive with *StratLearn*, which obtained a target AUC of 0.958. In fact, using IWCV alone leads to a decrease in performance for NN (0.897) and IPS (0.897) relative to the ‘Biased’ fit (0.902). In order to reweight the loss of each object separately when implementing IWCV, we optimize with respect to the log-loss instead of AUC. We do not expect this to be responsible for the decreased target performance. For example, using log-loss as the hyperparameter selection criterion for *StratLearn* in each source group (instead of AUC) leads to the same target AUC of 0.958. Importance sampling is the only weighting method for which we present the associated ROC curve in Figure 3, because it has the highest average AUC.

Covariate Balance on Updated SPCC Data:

Table S2 presents the covariate balance on the updated SPCC data before stratification (“raw” data), and after stratification via STACCATO and *StratLearn*, respectively.

On the non-stratified “raw” data, we measure an average (SD) SMD of 0.114 (0.202) across the 102 covariates, with an average (SD) KS-stats of 0.187 (0.084). *StratLearn* leads to increased balance within strata, strongly reducing the average

Table S2: Average (SD) of SMD and KS-stats computed on the observed covariates from the updated SPCC data (diffusion map coordinates, redshift and brightness) on “raw” data, and in strata built by *StratLearn* and STACCATO, respectively. Strata 3-5 are not displayed due to a shortage of source data. Smaller values indicate better balance.

	“raw” data	STACCATO		<i>StratLearn</i>	
		Stratum 1	Stratum 2	Stratum 1	Stratum 2
SMD	0.114 (0.202)	0.053 (0.039)	0.189 (0.195)	0.034 (0.028)	0.103 (0.161)
KS-stats	0.187 (0.084)	0.074 (0.05)	0.206 (0.093)	0.056 (0.048)	0.131 (0.08)

(SD) SMD to 0.034 (0.028) in stratum 1; KS-stats: 0.056 (0.048); and to an average (SD) SMD of 0.103 (0.161); KS-stats: 0.131 (0.08); in stratum 2. (The remaining strata contain too few source data to assess covariate balance.)

On average (SD) across all covariates, STACCATO led to an SMD of 0.053 (0.039); KS-stats: 0.074 (0.05), in stratum 1, and an average (SD) SMD of 0.189 (0.195), KS-stats: 0.206 (0.093), in stratum 2, much higher than *StratLearn*.

S6 StratLearn applied to original SPCC Data

This section provides additional numerical evidence for *StratLearn*, performing SNIa classification on the original “Supernova photometric classification challenge” (SPCC) data set provided by (Kessler et al., 2010), an earlier version of the SPCC data described in Section 4.2.

Data:

The application of *StratLearn* on the original SPCC data is mainly for comparison with previous literature that use this data set. The earlier version of the SPCC data features a total of 17,330 simulated SNe of type Ia (SNIa), Ib, Ic and II. The data set is divided into a source (training) set D_S of 1217 spectroscopically confirmed SNe with known types, and (target set) D_T of 16,113 SNe with unknown types and only photometric information. The simulation used to generate the original SPCC data suffered from a bug that made classification easier, thus leading to the updated SPCC data used in Section 4.2. As in Section 4.2, we applied GP fitting and diffusion maps (Revsbech et al., 2018; Richards et al., 2012) to obtain a set of 102 predictive covariates; 100 covariates from the diffusion map, plus redshift (defined in Section 4.3) and a measure of the objects’ brightness (Revsbech et al., 2018).

Results:

Table S3 presents the composition of the five strata obtained by conditioning on the estimated propensity scores, exhibiting a similar pattern as the strata composition on the updated SPCC data (Table 1), though with a higher proportion of SNIa in the first stratum and even less source data in strata 3 – 5. We thus follow the same strategy as described in Section 4.2. After stratification, a random forest classifier is trained and optimized on source strata D_{S_1} and D_{S_2} separately to classify SNe in target strata D_{T_1}

Table S3: Composition of the five strata on the original SPCC data (Kessler et al., 2010). The number of SNe, as well as the number and proportion of SNIa are presented in each source and target stratum.

Stratum	Set	Number of SNe	Number of SNIa	Prop. of SNIa
1	Source	996	794	0.80
	Target	2470	1759	0.71
2	Source	210	56	0.27
	Target	3256	1010	0.31
3	Source	9	0	0
	Target	3457	385	0.11
4	Source	2	1	0.50
	Target	3464	258	0.07
5	Source	0	0	NA
	Target	3466	180	0.05

and D_{T_2} , respectively. Source strata D_{S_j} for $j \in \{3, 4, 5\}$ are merged with D_{S_2} to train the random forest to predict D_{T_j} for $j \in \{3, 4, 5\}$. Repeated 10-fold cross validation (with the hyperparameter grid described in Section S5) is performed to minimize the empirical risk of (9) within each group.

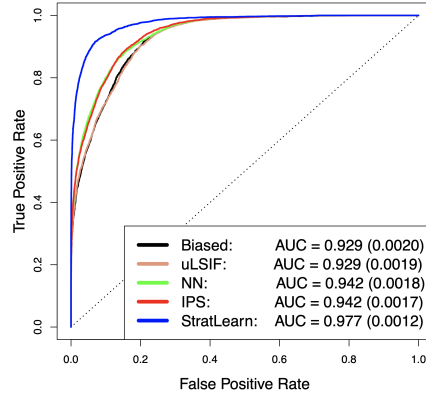


Fig. S1: Comparison of ROC curves for SNIa classification using the original SPCC data (Kessler et al., 2010). Bootstrap AUC standard errors (from 400 bootstrap samples) are presented in parenthesis.

With *StratLearn* we obtain an AUC of 0.977 on the target data of the original SPCC data (blue ROC curve in Figure S1), very near the optimal ‘gold standard’ benchmark, which is 0.981 on this data set (obtained on a set with 1217 objects randomly selected from the target data as a representative source set, which would not exhibit covariate shift and would not be available in practice). The AUC obtained with *StratLearn* is also larger than the previous best published AUC for this data, AUC =

Table S4: AUC results on the original SPCC (photometric) target data (Kessler et al., 2010), using various importance weighting approaches to adjust for covariate shift.

	IWCV	importance sampling	IWCV + importance sampling
uLSIF	0.934	0.929	0.936
NN	0.934	0.942	0.931
IPS	0.934	0.942	0.931

0.961 (Revsbech et al., 2018) with STACCATO, which employs a data augmentation strategy and target data leakage. Note that the predictive target performance on the original SPCC data (Kessler et al., 2010) is generally higher than on the updated version (Kessler et al., 2010), due to the aforementioned bug that made classification easier.

Most of the importance weighting methods (Table S4) lead to slight improvements over the (non-adjusted) ‘Biased’ model fit. The best performing weighting approaches (using estimated NN or IPS weights for importance sampling) obtain a target AUC of 0.942, substantially lower than *StratLearn* (AUC: 0.977). Importance sampling is the only weighting method for which we present the associated ROC curve in Figure S1, because it has the highest average AUC.

S6.1 Covariate Balance Check on Original SPCC Data

In this section, we illustrate the balancing property of propensity scores by assessing the covariate balance in the original SPCC data within strata conditional on the estimated propensity scores, such as described in the last paragraph of Section 3. In particular, we show that such balance assessment could be helpful to assess the suitability of choice of covariates and/or the propensity score model.

As mentioned in Section 4.2, the method proposed by Revsbech et al. (2018) (STACCATO) can be viewed as a prototype of *StratLearn*, as it augments the spectroscopic source data separately in strata based on the estimated propensity scores. STACCATO employs two covariates (“redshift” and measure of brightness) as main effects in a logistic regression model to estimate the propensity scores. In contrast, *StratLearn* includes all 100 diffusion map covariates (Section 4.2), in addition to “redshift” and “brightness”, as main effects in a logistic regression model to estimate the propensity scores. We assess the balance achieved through stratification by means of two commonly used balance measures: absolute standardized mean differences and the Kolmogorov-Smirnov test statistics (Austin, 2011; Mccaffrey et al., 2013), computed for each covariate within strata. Table S5 shows that, on average across observed covariates, *StratLearn* leads to substantially reduced absolute standardized mean differences and Kolmogorov-Smirnov test statistics in strata one and two, compared to STACCATO. We only report balance measures in strata one and two because of a shortage of source data in the remaining strata. Thus, building the strata by conditioning on the *StratLearn* estimated propensity scores leads to improved covariate balance (i.e., reduced covariate shift) within strata, compared to using the STACCATO estimated propensity scores. Notably, comparing the predictive performance, STACCATO

Table S5: Average (SD) of SMD and KS-stats computed on the observed covariates from the original SPCC data (diffusion map coordinates, redshift and brightness) on “raw” data, and in strata built by *StratLearn* and STACCATO, respectively. Strata 3-5 are not displayed due to a shortage of source data. Smaller values indicate better balance.

	“raw” data	<i>StratLearn</i>		STACCATO	
		Stratum 1	Stratum 2	Stratum 1	Stratum 2
SMD	0.126 (0.184)	0.031 (0.026)	0.066 (0.121)	0.057 (0.055)	0.132 (0.127)
KS-stats	0.186 (0.073)	0.053 (0.019)	0.095 (0.053)	0.084 (0.027)	0.163 (0.066)

(without augmentation) yields a target AUC of 0.942, whereas with *StratLearn* we obtain an AUC of 0.977 on the target data – a substantial improvement resulting from the improved covariate balance by accounting for potentially confounding covariates.

For illustration purposes, in Figure S2 we display a more detailed balance check, comparing the absolute standardized mean differences computed for each covariate in stratum 1 (obtained through *StratLearn* (black) and STACCATO (red)) with the absolute standardized mean differences of the covariates without stratification. In general, points below the diagonal line indicate better balance in the stratum compared to the balance on the ‘raw’ non-stratified data. Even though Revsbech et al. (2018) (STACCATO) just include redshift and brightness in the propensity score estimation, both approaches balance the majority of the covariates. However, the black (*StratLearn*) standardized mean differences have visibly smaller values in the y-direction, indicating better balance compared to the approach in Revsbech et al. (2018) (red). Note that for clarity of Figure S2, we removed one outlier (brightness) with a raw standardized mean difference of 1.5, which was very well balanced with a standardized mean difference of around 0.09 in stratum 1 by both approaches. Assessing the balance of individual covariates as illustrated in Figure S2 might be particularly useful to evaluate (and improve) the resulting balance of covariates important for outcome prediction. Some domain-specific expertise might be necessary to identify such covariates. In Section S7, we show how covariate balance assessment can be employed to evaluate the propensity score model choice.

Table S6 presents balance comparisons between STACCATO and *StratLearn* via predicted outcome labels (as described in Section 3.3). *StratLearn* leads to much better balance between predicted outcome proportions within strata one and two, and thus to much higher p-values than STACCATO, implying a much weaker relation between source/target assignment and predicted outcomes. The comparison of predicted outcome proportions and p-values (between *StratLearn* and STACCATO) provide a straightforward indication to employ the *StratLearn* propensity score model for stratification, which in turn leads to much improved outcome model predictive performance of SN1a classification.

S7 *StratLearn* applied to Data from UCI Repository

In this section, we demonstrate the performance of *StratLearn* under violation of the covariate shift assumption. We apply *StratLearn* on two datasets from the publicly

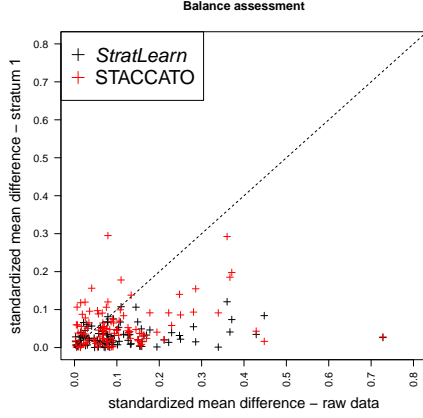


Fig. S2: Absolute standardized mean differences between source and target data of stratum 1 plotted against raw data absolute standardized mean differences for both propensity score (PS) estimation approaches (*StratLearn* and STACCATO). For visual clarity we left out one covariate which would appear at the coordinates (1.5,0.09).

Table S6: Outcome balance diagnostics via predicted labels on the original SPCC data (Section S6), applying STACCATO (left) and *StratLearn* (right). The number and proportion of predicted SNIa are presented in source and target stratum 1 and 2. P-values are computed via Fisher’s exact test of independence between predicted SNIa target and source proportions within strata.

Stratum	Set	STACCATO (predicted)			<i>StratLearn</i> (predicted)		
		Number of SNIa	Prop. of SNIa	p-value	Number of SNIa	Prop. of SNIa	p-value
1	Source	652	0.69	5.0e-21	794	0.80	0.013
	Target	1290	0.51		1872	0.76	
2	Source	181	0.74	6.9e-23	56	0.27	0.016
	Target	1336	0.41		1132	0.35	

available UCI repository (Dua and Graff, 2017): the “wine quality data” (Cortez et al., 2009) and the “Parkinson Telemonitoring data” (Little et al., 2008). These datasets have previously been used to explore regression problems in the presence of covariate shift (Chen et al., 2016). Links to these data sets can be found in Section S4.

S7.1 Data Description

Wine Quality Data:

The data set contains 6497 samples of which 4898 are of type “white wine”, used as source data D_S , and 1599 samples are of type “red wine”, used as the target data D_T . The output is a wine “quality score” (between 0 and 10), which we aim to predict for

the target data (red wine), given the scores of the source data (white wine). There are 11 physicochemical, predictive covariates. We refer to Cortez et al. (2009) for detailed information.

Parkinson Data:

The data comprises 5875 instances and 26 attributes. Similar to Chen et al. (2016), we take 17 of the attributes to be predictive covariates, with the aim of predicting the UPDRS Parkinson’s disease symptom score (output). The source data D_S contains all instances with age below 60, leading to a source subset of size $|D_S| = 1877$. Instances with age above (inclusively) 60 and below 70 are used as target samples D_T , with $|D_T| = 2127$. As in Chen et al. (2016), instances with age above 70 are not considered. We refer to Little et al. (2008) for further information on the data.

S7.2 Implementation and Results on UCI Data

Following Chen et al. (2016), our objective is to predict the wine “quality score” and the Parkinson’s “UPDRS” score using linear regression models, specifically ordinary least squares (OLS). We assume that the source and target splitting covariates (wine type and age) are not observed for model fitting. Note that, because these are confounding covariates, this violates the covariate shift assumption. All other available covariates are used to estimate the propensity scores and the importance weights, and as predictor variables for the outcome models. To improve covariate balance on the wine quality data, we use gradient boosting machines to estimate the propensity scores, commonly used in the propensity score causal inference literature (McCaffrey et al., 2004; Mccaffrey et al., 2013; Autenrieth et al., 2021). Covariate balance is assessed as described in the last paragraph of Section 3. On the wine quality data, we assess the covariate balance in stratum 4, which is the only stratum with both source and target samples (Table S7). Using logistic regression, the average (SD) absolute standardized mean difference in the observed covariate set is 0.667 (0.436), and the average (SD) of the Kolmogorov-Smirnov test statistics is 0.388 (0.154). Estimating the propensity scores using gradient boosting machines increases balance in stratum 4, by reducing the average (SD) absolute standardized mean difference to 0.561 (0.292), and the average (SD) Kolmogorov-Smirnov test statistics to 0.288 (0.109). On the Parkinson data set, logistic regression is used to estimate the propensity scores because it leads to better balance in the strata than using gradient boosting machines.

Table S7 presents the composition of the *StratLearn* strata for the Wine and Parkinson data, both conditioned on the estimated propensity scores. For the wine data set, all target samples are in strata 4 and 5, and only stratum 4 contains both source and target samples. Following our *StratLearn* strategy, we fit OLS on D_{S_4} to predict D_{T_4} and D_{T_5} . In the Parkinson data set there is enough source data in each strata to fit OLS separately on each source stratum D_{S_j} to predict the data in the respective target stratum D_{T_j} , $j \in \{1, \dots, 5\}$.

Table S8 presents the MSE of the target predictions, comparing *StratLearn* with (non-adjusted) OLS (‘Biased’) and WLS, using the methods described in Section 4.1 to estimate the weights. Applying *StratLearn* results in a target MSE of 0.715 for the Wine data and 114.97 for the Parkinson data, both improving upon the ‘Biased’ OLS

Table S7: Composition of the five *StratLearn* strata for the UCI wine and UCI parkinson data. The number of samples/subjects in source and target stratum, as well as the mean outcome (“quality score” and “UPDRS score”) are presented.

Stratum	Set	UCI Wine data	UCI Parkinson data
		# samples (Mean “quality”)	# subjects (Mean “UPDRS”)
1	Source	1299 (5.98)	627 (22.00)
	Target	0 (0.00)	174 (29.15)
2	Source	1300 (5.92)	486 (26.36)
	Target	0 (0.00)	315 (25.21)
3	Source	1300 (5.93)	314 (25.53)
	Target	0 (0.00)	487 (24.86)
4	Source	999 (5.63)	269 (27.38)
	Target	301 (5.49)	532 (28.15)
5	Source	0 (0.00)	181 (27.06)
	Target	1298 (5.67)	619 (30.00)
All	Source	4898 (5.88)	1877 (24.98)
	Target	1599 (5.64)	2127 (27.58)

fit which yields a target MSE of 1.024 (Wine) and 130.88 (Parkinson). *StratLearn* further provides better results than WLS:uLSIF, WLS:KLIEP and WLS:NN on both data sets; only WLS:IPS leads to slightly better results than *StratLearn*.

We also compare *StratLearn* with the method that Chen et al. (2016) develops and illustrates on these datasets. Specifically, Chen et al. (2016) proposes a “robust bias-aware regression” based on the Kullback-Leibler divergence. This proposal is tailored specifically to regression and to loss functions that account for uncertainty in the prediction (e.g., empirical logloss), whereas *StratLearn* is entirely general but can be successfully applied to this task. Following Chen et al. (2016), we compute the target empirical logloss as a performance measure. On the Wine data, *StratLearn* yields an empirical logloss of 1.271, which exactly matches the reported performance of the method proposed in Chen et al. (2016). On the Parkinson data we could not replicate the exact data split as reported in Chen et al. (2016), and thus a meaningful comparison of empirical logloss to the values reported by Chen et al. (2016) is not possible.

In summary, in these illustrative regression examples *StratLearn* demonstrates certain robustness against violation of the covariate shift assumption, improving upon the (non-adjusted) ‘Biased’ fit and performing comparably with the best importance weighting approach.

S8 Additional Results for Redshift Regression

In the context of the photometric redshift regression example in Section 4.3, we present additional numerical results that demonstrate the robustness of *StratLearn* to varying degrees of covariate shift. Specifically, we reproduce the results of Section 4.3, but under two additional covariate shift scenarios.

Table S8: MSE of target predictions on UCI Wine and Parkinson data, based on ordinary least squares regression (OLS), various importance weighted least squares regression methods (WLS), and our proposed *StratLearn* method.

Method \ Data	UCI wine data	UCI Parkinson data
OLS (Biased)	1.024	130.88
WLS:uLSIF	2.363	120.81
WLS:KLIEP	3.968	116.72
WLS:NN	2.377	117.47
WLS:IPS	0.660	112.80
StratLearn	0.715	114.97

Additional Covariate Shift Setups:

We use the same data setup as in Section 4.3, but change the rejection sampling used to simulate an unrepresentative target D_T from D_S , to

- Weak covariate shift:

$$p(s=0|x) = f_{B(9,4)}(x_{(r)}) / \max_{x_{(r)}} f_{B(9,4)}(x_{(r)}) \quad (24)$$

- Strong covariate shift:

$$p(s=0|x) = f_{B(18,4)}(x_{(r)}) / \max_{x_{(r)}} f_{B(18,4)}(x_{(r)}), \quad (25)$$

where $x_{(r)}$ is the r -band magnitude and $f_{B(9,4)}$ and $f_{B(18,4)}$ are beta densities with parameters (9,4) and (18,4), respectively. Except for the adjusted degree of covariate shift, simulations are performed as described in Section 4.3.

Summary – Conditional Density Estimation:

Figure S3 compares the resulting target risk $\hat{R}_T(\hat{f})$ across models and covariate sets, for the weak covariate shift (top row) and the strong covariate shift scenario (bottom row). These results, combined with those from the medium covariate shift scenario in Figure 5, reinforce the advantage of using *StratLearn*, especially for higher dimensional covariate sets. In Figures 5 and S3, *StratLearn_{Series}* performs well in the setup with the fewest covariates (left column). In the weak covariate shift scenario, this leads to an additional boost in performance of *StratLearn_{Comb}* (which combines *StratLearn_{ker-NN}* and *StratLearn_{Series}*, following (12)). In the setups with higher dimensional covariates, the Series methods (using either *StratLearn* or the weighting methods) exhibit relatively poor performance overall. In these cases, the *StratLearn_{Comb}* predictions rely solely on *StratLearn_{ker-NN}*, which again demonstrates the successful empirical risk minimization of (9), inasmuch as *StratLearn_{Comb}* automatically selects the better *target* model (i.e., *StratLearn_{ker-NN}*) in each stratum, based on the respective empirical *source* risk estimates in each stratum. Overall, IPS and NN weighting are most competitive with *StratLearn*, in addition to KLIEP in the low dimensional, strong covariate shift setup. Note that the performances of *IPS_{Comb}*, *KLIEP_{Comb}* and *uLSIF_{Comb}* are

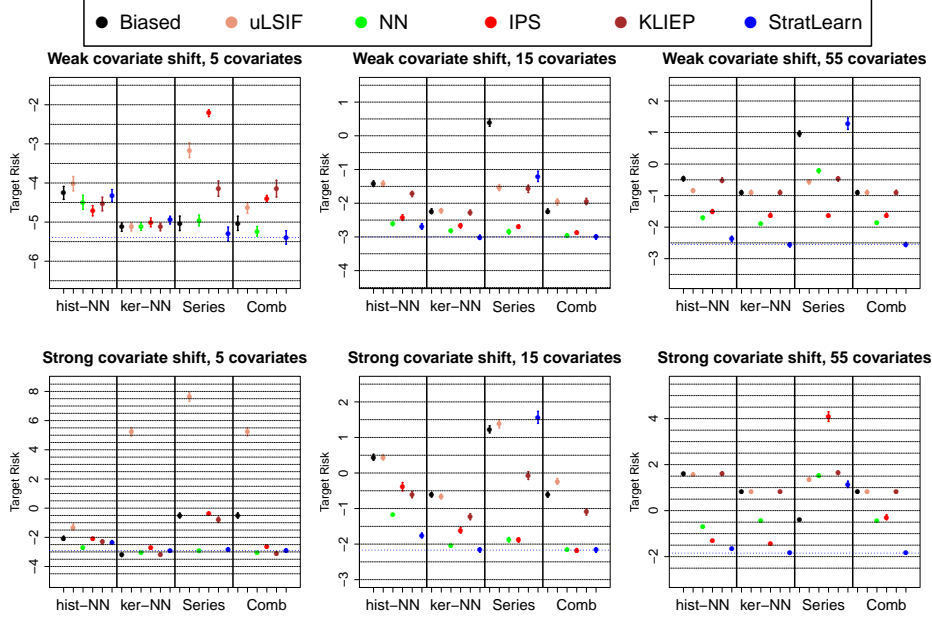


Fig. S3: Target risk (\hat{R}_T) of the four photo- z estimation models under each method (different colors), using different sets of predictors. Bars give the mean ± 2 bootstrap standard errors (from 400 bootstrap samples). Top row: Weak covariate shift (following (24)); Bottom row: Strong covariate shift (following (25)).

Table S9: Composition of the five *StratLearn* strata for the medium covariate shift scenario (as described in Section 4.3) on SDSS data, using estimated propensity scores with different sets of predictors. The number of galaxies in source and target stratum, as well as the mean outcome (redshift z) are presented.

Stratum	Set	5 covariates	15 covariates	55 covariates
		#galaxies (Mean z)	#galaxies (Mean z)	#galaxies (Mean z)
1	Source	1631 (0.09)	1583 (0.09)	1620 (0.09)
	Target	7 (0.07)	9 (0.07)	7 (0.07)
2	Source	1500 (0.13)	1515 (0.13)	1546 (0.13)
	Target	112 (0.11)	113 (0.13)	98 (0.11)
3	Source	618 (0.29)	641 (0.29)	594 (0.30)
	Target	1481 (0.33)	1499 (0.33)	1480 (0.33)
4	Source	116 (0.42)	114 (0.40)	108 (0.40)
	Target	2196 (0.39)	2215 (0.38)	2258 (0.38)
5	Source	135 (0.48)	147 (0.46)	132 (0.47)
	Target	2204 (0.48)	2164 (0.48)	2157 (0.48)
All	Source	4000 (0.16)	4000 (0.16)	4000 (0.16)
	Target	6000 (0.40)	6000 (0.40)	6000 (0.40)

Table S10: Composition of the five *StratLearn* strata for the weak covariate shift (24) and strong covariate shift (25) scenarios on SDSS data, using a set of five predictors for propensity score estimation. The number of galaxies in source and target stratum, as well as the mean outcome (redshift z) are presented.

Stratum	Set	weak covariate shift, 5 covariates	strong covariate shift, 5 covariates
		#galaxies (Mean z)	#galaxies (Mean z)
1	Source	1468 (0.09)	1603 (0.07)
	Target	145 (0.09)	0 (NaN)
2	Source	1220 (0.13)	1579 (0.10)
	Target	602 (0.11)	4 (0.10)
3	Source	740 (0.20)	637 (0.24)
	Target	1275 (0.21)	1494 (0.28)
4	Source	301 (0.37)	73 (0.36)
	Target	1958 (0.37)	2297 (0.33)
5	Source	271 (0.47)	108 (0.41)
	Target	2020 (0.44)	2205 (0.37)
All	Source	4000 (0.17)	4000 (0.13)
	Target	6000 (0.33)	6000 (0.34)

degraded in some cases (e.g., Figure S3, upper left panel) with inclusion of the poorly performing *Series* predictions, illustrating that the weighted empirical *source* risk minimization ((11), as a form of (1)) does not lead to *target* risk minimization in these situations. With increasing number of covariates, none of the weighted models yield results that are competitive with *StratLearn*.

Table S9 presents the composition of the five *StratLearn* strata for the medium covariate shift scenario (described in Section 4.3) for each of the three sets of covariates. Each source stratum contains a sufficient sample size to fit the conditional density estimators for prediction on the respective target stratum. The overall redshift averages in the source (0.11) and target data (0.28) are very unequal, a consequence of the covariate shift. Within strata, the redshift averages are well aligned between source and target, indicating improved balance after stratification. Notably, the composition of the strata in the high-dimensional covariate setup is similar to the that of the lower-dimensional setups, with well-balanced strata. This is an indication of the robustness of *StratLearn* with respect to high dimensional (noisy) sets of covariates. Table S10 compares the five *StratLearn* strata for the weak and strong covariate shift scenarios, again with well-aligned average redshift within each stratum. Note that for the strong covariate shift scenario there are almost no galaxies in the first two target strata. Thus, effectively only data in source stratum 3 to 5 are used for target prediction in the respective strata. These examples illustrate the advantage of using only a small subset of the source data when formulating predictions for individuals in the target, where the subset is chosen for its similarity to the target data in question. This is a markedly different strategy to the widespread practice of including all possible available data when fitting machine learning models.

Supplementary References

- Allam Jr, T., Bahmanyar, A., Biswas, R., Dai, M., Galbany, L., Hložek, R., Ishida, E. E., Jha, S. W., Jones, D. O., Kessler, R. et al. (2018), “The photometric lsst astronomical time-series classification challenge (plasticc): Data set,” *arXiv preprint arXiv:1810.00001*.
- Austin, P. C. (2011), “An introduction to propensity score methods for reducing the effects of confounding in observational studies,” *Multivariate behavioral research*, 46, 399–424.
- Austin, P. C., and Stuart, E. A. (2015), “Moving towards best practice when using inverse probability of treatment weighting (IPTW) using the propensity score to estimate causal treatment effects in observational studies,” *Statistics in medicine*, 34, 3661–3679.
- Autenrieth, M., Levine, R. A., Fan, J., Guarcello, M. A. et al. (2021), “Stacked Ensemble Learning for Propensity Score Methods in Observational Studies,” *Journal of Educational Data Mining*, 13, 24–189.
- Baktashmotlagh, M., Harandi, M. T., Lovell, B. C., and Salzmann, M. (2014), “Domain adaptation on the statistical manifold,” in *Proceedings of the IEEE conference on computer vision and pattern recognition*, pp. 2481–2488.
- Bekker, J., Robberechts, P., and Davis, J. (2019), “Beyond the selected completely at random assumption for learning from positive and unlabeled data,” in *Joint European Conference on Machine Learning and Knowledge Discovery in Databases*, Springer, pp. 71–85.
- Ben-David, S., Blitzer, J., Crammer, K., Kulesza, A., Pereira, F., and Vaughan, J. W. (2010), “A theory of learning from different domains,” *Machine learning*, 79, 151–175.
- Ben-David, S., Blitzer, J., Crammer, K., Pereira, F. et al. (2007), “Analysis of representations for domain adaptation,” *Advances in neural information processing systems*, 19, 137.
- Bickel, S., Brückner, M., and Scheffer, T. (2009), “Discriminative learning under covariate shift,” *Journal of Machine Learning Research*, 10, 2137–2155.
- Bickel, S.— (2007), “Dirichlet-enhanced spam filtering based on biased samples,” in *Advances in neural information processing systems*, pp. 161–168.
- Bruzzzone, L., and Marconcini, M. (2009), “Domain adaptation problems: A DASVM classification technique and a circular validation strategy,” *IEEE transactions on pattern analysis and machine intelligence*, 32, 770–787.

- Chen, X., Monfort, M., Liu, A., and Ziebart, B. D. (2016), “Robust covariate shift regression,” in *Artificial Intelligence and Statistics*, PMLR, pp. 1270–1279.
- Cortes, C., Mansour, Y., and Mohri, M. (2010), “Learning bounds for importance weighting,” in *Advances in neural information processing systems*, pp. 442–450.
- Cortes, C., Mohri, M., Riley, M., and Rostamizadeh, A. (2008), “Sample selection bias correction theory,” in *International conference on algorithmic learning theory*, Springer, pp. 38–53.
- Cortez, P., Cerdeira, A., Almeida, F., Matos, T., and Reis, J. (2009), “Modeling wine preferences by data mining from physicochemical properties,” *Decision support systems*, 47, 547–553.
- Courty, N., Flamary, R., Habrard, A., and Rakotomamonjy, A. (2017), “Joint distribution optimal transportation for domain adaptation,” *arXiv preprint arXiv:1705.08848*.
- Courty, N., Flamary, R., Tuia, D.— (2016), “Optimal transport for domain adaptation,” *IEEE transactions on pattern analysis and machine intelligence*, 39, 1853–1865.
- Csurka, G. (2017), “A comprehensive survey on domain adaptation for visual applications,” *Domain adaptation in computer vision applications*, 1–35.
- Dua, D., and Graff, C. (2017), “UCI Machine Learning Repository,” .
- Fernando, B., Habrard, A., Sebban, M., and Tuytelaars, T. (2013), “Unsupervised visual domain adaptation using subspace alignment,” in *Proceedings of the IEEE international conference on computer vision*, pp. 2960–2967.
- Franklin, J. M., Rassen, J. A., Ackermann, D., Bartels, D. B., and Schneeweiss, S. (2014), “Metrics for covariate balance in cohort studies of causal effects,” *Statistics in medicine*, 33, 1685–1699.
- Freeman, P. E., Izbicki, R., and Lee, A. B. (2017), “A unified framework for constructing, tuning and assessing photometric redshift density estimates in a selection bias setting,” *Monthly Notices of the Royal Astronomical Society*, 468, 4556–4565.
- Gieseke, F., Polsterer, K. L., Thom, A., Zinn, P., Bomanns, D., Dettmar, R.-J., Kramer, O., and Vahrenhold, J. (2010), “Detecting quasars in large-scale astronomical surveys,” in *2010 Ninth International Conference on Machine Learning and Applications*, IEEE, pp. 352–357.
- Gong, B., Grauman, K., and Sha, F. (2013), “Reshaping visual datasets for domain adaptation,” *Advances in Neural Information Processing Systems*, 26, 1286–1294.

- Gong, M., Zhang, K., Liu, T., Tao, D., Glymour, C., and Schölkopf, B. (2016), “Domain adaptation with conditional transferable components,” in *International conference on machine learning*, PMLR, pp. 2839–2848.
- Griffin, B. A., McCaffrey, D. F., Almirall, D., Burgette, L. F., and Setodji, C. M. (2017), “Chasing balance and other recommendations for improving nonparametric propensity score models,” *Journal of causal inference*, 5.
- Hassanpour, N., and Greiner, R. (2019), “Counterfactual regression with importance sampling weights,” in *Proceedings of the Twenty-Eighth International Joint Conference on Artificial Intelligence, IJCAI-19*, pp. 5880–5887.
- Hirano, K., Imbens, G. W., and Ridder, G. (2003), “Efficient estimation of average treatment effects using the estimated propensity score,” *Econometrica*, 71, 1161–1189.
- Hoffman, J., Wang, D., Yu, F., and Darrell, T. (2016), “Fcns in the wild: Pixel-level adversarial and constraint-based adaptation,” *arXiv preprint arXiv:1612.02649*.
- Imai, K., and Ratkovic, M. (2014), “Covariate balancing propensity score,” *Journal of the Royal Statistical Society: Series B (Statistical Methodology)*, 76, 243–263.
- Imai, K., and van Dyk, D. A. (2004), “Causal inference with general treatment regimes: Generalizing the propensity score,” *Journal of the American Statistical Association*, 99, 854–866.
- Jiang, J., and Zhai, C. (2007), “Instance weighting for domain adaptation in NLP,” *ACL*.
- Joachims, T., Swaminathan, A., and Schnabel, T. (2017), “Unbiased learning-to-rank with biased feedback,” in *Proceedings of the Tenth ACM International Conference on Web Search and Data Mining*, ACM, pp. 781–789.
- Kamnitsas, K., Baumgartner, C., Ledig, C., Newcombe, V., Simpson, J., Kane, A., Menon, D., Nori, A., Criminisi, A., Rueckert, D. et al. (2017), “Unsupervised domain adaptation in brain lesion segmentation with adversarial networks,” in *International conference on information processing in medical imaging*, Springer, pp. 597–609.
- Kanamori, T., Hido, S., and Sugiyama, M. (2009), “A least-squares approach to direct importance estimation,” *Journal of Machine Learning Research*, 10, 1391–1445.
- Kanamori, T., Suzuki, T.— (2012), “Statistical analysis of kernel-based least-squares density-ratio estimation,” *Machine Learning*, 86, 335–367.
- Kouw, W. M., and Loog, M. (2019), “A review of domain adaptation without target labels,” *IEEE transactions on pattern analysis and machine intelligence*.

- Kouw, W. M., Van Der Maaten, L. J., Krijthe, J. H.— (2016), “Feature-level domain adaptation,” *The Journal of Machine Learning Research*, 17, 5943–5974.
- Kuhn, M. (2008), “Building Predictive Models in R Using the caret Package,” *Journal of Statistical Software, Articles*, 28, 1–26.
- Lee, B. K., Lessler, J., and Stuart, E. A. (2010), “Improving propensity score weighting using machine learning,” *Statistics in medicine*, 29, 337–346.
- Little, M., McSharry, P., Hunter, E., Spielman, J., and Ramig, L. (2008), “Suitability of dysphonia measurements for telemonitoring of Parkinson’s disease,” *Nature Precedings*, 1–1.
- Liu, A., and Ziebart, B. D. (2014), “Robust Classification Under Sample Selection Bias.” in *NIPS*, pp. 37–45.
- Lunceford, J. K., and Davidian, M. (2004), “Stratification and weighting via the propensity score in estimation of causal treatment effects: a comparative study,” *Statistics in medicine*, 23, 2937–2960.
- Magliacane, S., van Ommen, T., Claassen, T., Bongers, S., Versteeg, P., and Mooij, J. M. (2018), “Domain adaptation by using causal inference to predict invariant conditional distributions,” in *Advances in Neural Information Processing Systems*, pp. 10846–10856.
- McCaffrey, D., Griffin, B. A., Almirall, D., Slaughter, M., Ramchand, R., and F Burgette, L. (2013), “A Tutorial on Propensity Score Estimation for Multiple Treatments Using Generalized Boosted Models,” 32.
- McCaffrey, D. F., Ridgeway, G., and Morral, A. R. (2004), “Propensity score estimation with boosted regression for evaluating causal effects in observational studies.” *Psychological methods*, 9, 403.
- Möller, A., and de Boissière, T. (2020), “SuperNNova: an open-source framework for Bayesian, neural network-based supernova classification,” *Monthly Notices of the Royal Astronomical Society*, 491, 4277–4293.
- Pan, S. J., Tsang, I. W., Kwok, J. T., and Yang, Q. (2010), “Domain adaptation via transfer component analysis,” *IEEE Transactions on Neural Networks*, 22, 199–210.
- Pan, S. J.— (2009), “A survey on transfer learning,” *IEEE Transactions on knowledge and data engineering*, 22, 1345–1359.
- Parast, L., McCaffrey, D. F., Burgette, L. F., de la Guardia, F. H., Golinelli, D., Miles, J. N. V., and Griffin, B. A. (2017), “Optimizing variance-bias trade-off in the TWANG package for estimation of propensity scores,” *Health Services and Outcomes Research Methodology*, 17, 175–197.

- Patel, V. M., Gopalan, R., Li, R., and Chellappa, R. (2015), “Visual domain adaptation: A survey of recent advances,” *IEEE signal processing magazine*, 32, 53–69.
- Pirracchio, R., and Carone, M. (2018), “The Balance Super Learner: A robust adaptation of the Super Learner to improve estimation of the average treatment effect in the treated based on propensity score matching,” *Statistical Methods in Medical Research*, 27, 2504–2518, PMID: 28339317.
- Pirracchio, R., Petersen, M. L., and van der Laan, M. (2014), “Improving propensity score estimators’ robustness to model misspecification using super learner,” *American journal of epidemiology*, 181, 108–119.
- Quionero-Candela, J., Sugiyama, M., Schwaighofer, A., and Lawrence, N. D. (2009), *Dataset shift in machine learning*, The MIT Press.
- R Core Team (2019), *R: A Language and Environment for Statistical Computing*, R Foundation for Statistical Computing, Vienna, Austria.
- Revsbech, E. A., Trotta, R., and van Dyk, D. A. (2018), “STACCATO: a novel solution to supernova photometric classification with biased training sets,” *Monthly Notices of the Royal Astronomical Society*, 473, 3969–3986.
- Rojas-Carulla, M., Schölkopf, B., Turner, R., and Peters, J. (2018), “Invariant models for causal transfer learning,” *The Journal of Machine Learning Research*, 19, 1309–1342.
- Schnabel, T., Swaminathan, A., Singh, A., Chandak, N., and Joachims, T. (2016), “Recommendations as treatments: Debiasing learning and evaluation,” in *international conference on machine learning*, PMLR, pp. 1670–1679.
- Setoguchi, S., Schneeweiss, S., Brookhart, M. A., Glynn, R. J., and Cook, E. F. (2008), “Evaluating uses of data mining techniques in propensity score estimation: a simulation study,” *Pharmacoepidemiology and drug safety*, 17, 546–555.
- Shimodaira, H. (2000), “Improving predictive inference under covariate shift by weighting the log-likelihood function,” *Journal of statistical planning and inference*, 90, 227–244.
- Stonnington, C. M., Tan, G., Klöppel, S., Chu, C., Draganski, B., Jack Jr, C. R., Chen, K., Ashburner, J., and Frackowiak, R. S. (2008), “Interpreting scan data acquired from multiple scanners: a study with Alzheimer’s disease,” *Neuroimage*, 39, 1180–1185.
- Stuart, E. A., Lee, B. K., and Leacy, F. P. (2013), “Prognostic score-based balance measures can be a useful diagnostic for propensity score methods in comparative effectiveness research,” *Journal of clinical epidemiology*, 66, S84–S90.

- Sugiyama, M., Nakajima, S., Kashima, H., Buenau, P. V., and Kawanabe, M. (2008), “Direct importance estimation with model selection and its application to covariate shift adaptation,” in *Advances in neural information processing systems*, pp. 1433–1440.
- Sugiyama, M., Oberwolfach, M. F., Kawanabe, M., and Chui, P. L. (2010), “Dimensionality Reduction for Density Ratio Estimation in High-dimensional Spaces,” *Neural Networks*, 23, 44–59.
- Sugiyama, M., Yamada, M., Von Buenau, P., Suzuki, T., Kanamori, T., and Kawanabe, M. (2011), “Direct density-ratio estimation with dimensionality reduction via least-squares hetero-distributional subspace search,” *Neural Networks*, 24, 183–198.
- Tai, L., Paolo, G., and Liu, M. (2017), “Virtual-to-real deep reinforcement learning: Continuous control of mobile robots for mapless navigation,” in *2017 IEEE/RSJ International Conference on Intelligent Robots and Systems (IROS)*, IEEE, pp. 31–36.
- Tsuboi, Y., Kashima, H., Hido, S., Bickel, S., and Sugiyama, M. (2009), “Direct density ratio estimation for large-scale covariate shift adaptation,” *Journal of Information Processing*, 17, 138–155.
- Van Opbroek, A., Ikram, M. A., Vernooij, M. W., and De Bruijne, M. (2014), “Transfer learning improves supervised image segmentation across imaging protocols,” *IEEE transactions on medical imaging*, 34, 1018–1030.
- Vilalta, R., Gupta, K. D., and Macri, L. (2013), “A machine learning approach to Cepheid variable star classification using data alignment and maximum likelihood,” *Astronomy and Computing*, 2, 46–53.
- Wen, J., Greiner, R., and Schuurmans, D. (2015), “Correcting covariate shift with the Frank-Wolfe algorithm,” in *Twenty-Fourth International Joint Conference on Artificial Intelligence*.
- Wen, J., Yu, C.-N., and Greiner, R. (2014), “Robust learning under uncertain test distributions: Relating covariate shift to model misspecification,” in *International Conference on Machine Learning*, PMLR, pp. 631–639.
- Westreich, D., Cole, S. R., Funk, M. J., Brookhart, M. A., and Stürmer, T. (2011), “The role of the c-statistic in variable selection for propensity score models,” *Pharmacoepidemiology and drug safety*, 20, 317–320.
- Yoon, J., Zhang, Y., Jordon, J., and van der Schaar, M. (2020), “VIME: Extending the Success of Self-and Semi-supervised Learning to Tabular Domain,” *Advances in Neural Information Processing Systems*, 33.

Yu, Y., and Szepesvári, C. (2012), “Analysis of kernel mean matching under covariate shift,” *arXiv preprint arXiv:1206.4650*.